CHARACTERIZING THE ROLES FOR HOST-DERIVED LIPIDS DURING MYCOBACTERIUM TUBERCULOSIS INFECTION

A Dissertation

Presented to the Faculty of the Graduate School

of Cornell University

In Partial Fulfillment of the Requirements for the Degree of

Doctor of Philosophy

by

Rachael Alexis Fieweger

August 2023

CHARACTERIZING THE ROLES FOR HOST-DERIVED LIPIDS DURING MYCOBACTERIUM TUBERCULOSIS INFECTION

Rachael Alexis Fieweger, Ph. D.

Cornell University 2023

Mycobacterium tuberculosis (Mtb), the causative agent of tuberculosis, is a proficient bacterial pathogen capable of establishing long-term infection in humans. An important factor contributing to the long-term survival of Mtb is its ability to utilize host-derived lipids both as an energy source and as precursors for biosynthesis of cell envelope lipids that act as essential virulence factors.

To take advantage of host nutrients, Mtb employs importers, Mce1 and Mce4, to facilitate uptake of fatty acids and cholesterol, respectively. These multiprotein complexes are hypothesized to utilize the same ATPase, MceG, to enable translocation of lipid substrates into the cytosol. Key shared subunits have been identified as essential for stabilizing the two transporters, therefore we investigated the role of MceG in stabilizing the Mce1 and Mce4 complexes. We show enzymatic activity of MceG is required for Mce1- and Mce4-mediated transport of fatty acids and cholesterol and that loss of lipid uptake in mutants lacking MceG is due to degradation of the complexes. Lastly, we show that MceG is required for full fitness in mice indicating that MceG may be a bottleneck that could be exploited by novel therapeutics.

Once imported, host lipids can be assimilated into Mtb lipid biosynthetic pathways to produce virulence factors that influence the host immune response and aid in the establishment of infection. One such immune response is dependent on prostaglandin E_2 (PGE_2), which regulates both cell death pathways and macrophage type I interferon (IFN) responses, yet how Mtb induces PGE_2 production remains poorly understood. Here, we demonstrate that the cell wall lipid, phthiocerol dimycocerosate (PDIM), is required to stimulate PGE_2 synthesis during Mtb infection in mice and in macrophages *ex vivo*. Additionally, PDIM-dependent stimulation of PGE_2 production occurs independent of signaling through IL-1β but requires export of the ESX-1 secretory protein, ESAT-6. Overall, this work reveals a new aspect of Mtb sensing in the cytosol of macrophages and provides a more complete understanding of critical events in lipid homeostasis during Mtb infection.

BIOGRAPHICAL SKETCH

Rachael Fieweger earned her Associates of Arts and Science degree from the University of Wisconsin—Fox Valley in 2014 and then her Bachelor of Science degree in Genetics from the University of Wisconsin—Madison in 2016. At UW-Madison, she worked as an undergraduate research assistant in the laboratory of Dr. Xuehua Zhong where she studied how epigenetic modifications of histones regulate development of *Arabidopsis thaliana*. In 2016, Rachael began her graduate studies in the Department of Microbiology at Cornell University where she joined the laboratory of Dr. Brian VanderVen and under his mentorship began studying lipid utilization pathways in *Mycobacterium tuberculosis*.

To

Florence and John

Robert and Rosemary

Anthony and Leigh Ann

ACKNOWLEDGMENTS

I would like to thank Dr. Brian VanderVen, my PhD advisor, for taking a chance on me when he welcomed me into the lab my first week on campus and then continuing to champion me unwaveringly during my PhD. I believe that time is one of the greatest gifts you can give someone, and Brian has never hesitated to make time for me in the lab. Thank you for always being willing to discuss the science, run countless experiments with me, and for teaching me all that you know with patience and encouragement. Thank you for always celebrating our successes, steadfastly supporting us no matter what arose, and for amusing us through it all with jokes, stories, and great music. I am endlessly grateful for your mentorship.

Additionally, I thank my committee members Dr. Joseph Peters and Dr. Tobias Doerr for their support both in the form of creative suggestions for new ways of thinking about my projects and in the form of guidance for how to navigate the ups and downs of graduate school. They could always be counted upon to hold space, meeting me wherever I was at with compassion, and for that I am grateful.

Thank you to my current and past lab mates, especially Christine Montague and Emma Roszkowski as they are two resilient, radiant women who have brought so much joy into my life. I cherish all the silly moments we share with each other, and I am grateful to have insightful and scrappy teammates to navigate the challenges with.

An additional, special thank you to Paul Jennette and the folks at Environmental Health & Safety for diligently making sure the BSL3 laboratories are working and for keeping us safe.

I would also like to thank those who I have met through participating in the Cornell Prison Education Program. To the administrators of the program, especially Keisha Slaughter and Betsye Violette, for giving me the opportunity to participate and being role models for how to lead a cause with both strength and compassion. To the students I have taught through the program, thank you for always bringing joy, vulnerability, and an eagerness for intellectual exchange to the classroom. It was truly an honor to teach through this program.

Furthermore, my academic journey would not have been possible without the guidance and support of my mentor at UW-Madison, Dr. Dean Sanders. I'm so grateful that in my first experience doing research I had a role model for what it means to be an upstanding and kind scientist. Dean's level-headedness, genuine nature, and generosity are traits I try to emulate every day.

Lastly, thank you to my family and loved ones who have made up my support system outside of the lab. I truly would not be here if it weren't for them. To my grandparents for being islands of unconditional love and safety. To Abigail Stark, for cultivating radiance in others, for being a grounding force in my life, and for teaching me to honor the "both/and" of life. To my parents for facilitating and fighting for my education, for always believing I can succeed, and for giving me the tools to do so. Your tenacity, adaptability, and endless love will always inspire me.

TABLE OF CONTENTS

LIST OF FIGURES

Chapter 1

Chapter 2

Chapter 3

Chapter 4

LIST OF TABLES

LIST OF ABBREVIATIONS

AA	arachidonic acid
ABC	ATP-binding cassette
BMMΦ	Bone marrow-derived macrophage
Bodipy-C16	Bodipy palmitate
CFU	Colony forming units
COX-2	cyclooxygenase-2
CSP	cytosolic surveillance pathway
DAT	diacyltrehalose
DMSO	dimethylsulfoxide
ΔMceG	MceG mutant in Mtb
ΔESAT-6	ESAT-6 mutant in Mtb
IFNs	Interferons
IL-1R	IL-1 receptor
LAM	lipoarabinomannans
ManLAM	mannose capped LAM
$mas^{Pro1223delC}$	mas point mutant
Mce	mammalian cell entry
MOI	Multiplicity of infection
Mtb	*Mycobacterium tuberculosis*
MTBC	*Mycobacterium tuberculosis* complex
NO	nitric oxide
PAT	polyacyltrehalose
PDIM	phthiocerol dimycocerosates
PDIM-	isolates lacking PDIM

PDIM+	isolates producing PDIM
PGE_2	prostaglandin E_2
PIMS	phosphatidylinositol mannosides
PRR	pattern recognition receptors
SLs	sulfolipids
TAG	triacylglycerol
TDM	trehalose dimycolate
TLC	thin-layer chromatography
TLR	toll-like receptors
TMM	trehalose monomycolate
TMT	tandem mass tag
WCL	whole cell lysates
WT	wild type

CHAPTER 1

Introduction

Mycobacterium tuberculosis: A 70,000-year-Old Companion

For thousands of years *Mycobacterium tuberculosis* (Mtb), the bacterial pathogen that causes tuberculosis, has been infecting the human population [1]. With humans as its only known natural reservoir, Mtb has co-evolved alongside its human host, honing its physiology to become a proficient pathogen. It is so successful that in 2021, Mtb newly infected 10.6 million people and led to the death of 1.6 million people across the globe [2]. One defining feature of Mtb pathogenesis is its ability to survive within its human host for years to decades before causing active TB disease and initiating transmission to a new host. As of 2018, about one-fifth of the world's population is latently infected with Mtb, and about ten percent of those infected will go on to develop active disease and therefore perpetuate the spread of this harmful bacteria [3].

With more than 170 species, the genus *Mycobacterium* has representatives abundant throughout environmental habitats including soil, swamps, peats, and sources of water in addition to humans and animals [4, 5]. It is generally thought that *M. tuberculosis* evolved from an ancient environmental Mycobacteria living in either an aquatic environment or the soil [4] and there is strong evidence that the initial colonization of humans with this ancient Mycobacteria took place in the horn of Africa, and the bacterium's spread and evolution was facilitated by humans' migration out of Africa [1, 6, 7]. Over time, it is likely that humans infected animals leading to the evolution of animal-adapted Mycobacterial pathogens while modern *M. tuberculosis* strains arose through co-evolution in humans [6]. Currently, the genus *Mycobacterium* is in the phylum Actinobacteria, and it contains non-pathogenic

species, opportunistic pathogens, and the *Mycobacterium tuberculosis* complex (MTBC) which consists of closely related obligate pathogens of humans and animals. Human adapted bacteria in the MTBC (*M. tuberculosis sensu stricto* and *M. africanum*) are comprised of seven phylogenetic lineages that continue to circulate in the human population, continuing to co-evolve alongside of us and further perfect their pathogenicity [8].

A crucial contributor to pathogenicity and a significant commonality between species of the MTBC is their ability to utilize host lipids. Not only are host-derived lipids a critical energy source, but they also provide precursors necessary for the biosynthesis of an array of unique lipids that Mtb incorporates into its cell envelope. The lipids present in the Mtb cell envelope provide protection as a thick hydrophobic barrier and through their interactions with the host immune system they help to ensure bacterial survival.

The Course of Mtb Infection

Mtb is transmitted through inhalation of aerosolized cough droplets and upon entering the lungs the bacteria is phagocytosed by resident macrophages where it inhibits phagosome-lysosome fusion and Mtb resides within a macrophage endosomal compartment [9]. The initial immune response involves the recruitment of innate immune cells, such as dendritic cells, neutrophils, monocytes, and macrophages, which can provide additional intracellular niches for Mtb. Some innate immune cells will under apoptosis resulting in bacterial clearance whereas others will undergo necrosis promoting bacterial dissemination [10]. Over time, antigen specific adaptive

immune cells such as T cells and B cells respond to the site of infection, and the accumulation of these immune cells at the site of infection confines the bacteria through the formation of a granuloma [11, 12]. Even though adaptive immune cells remain at the periphery of the granuloma, CD4 T_H cells are still important for containing the infection as they release IFN-γ which stimulates critical antimicrobial defenses in macrophages such as inducing nitric oxide (NO) production [13]. While Mtb can predominantly be found living intracellularly in macrophages located in the granuloma, the bacteria can also gain access to the macrophage cytosol through permeabilization of the phagosome and the bacteria can also reside extracellularly in the acellular center of necrotic granulomas, an environment consisting of caseum which is enriched with cellular debris and host-derived lipids [14-16].

The host immune system responds to Mtb infection through the production of many important cytokines and signaling molecules. Innate immune cells detect Mtb through pattern recognition receptors (PRRs), such as toll-like receptors (TLR) and C-type lectin receptors, and recognition via these receptors induces production of inflammatory cytokines such as TNF, IL-6, and IL-1β through NF-κB signaling and these mediators are generally host-protective [17]. Inflammation and IL-1β signaling also promotes production of eicosanoids, such as prostaglandin E_2 (PGE_2), which can promote or suppress the inflammatory response [18]. PGE_2 is produced when arachidonic acid stored in cell membranes is released by phospholipases A_2 and metabolized into PGE_2 via cyclooxygenases (COX). PGE_2 production induces apoptosis of infected macrophages and bacterial clearance during early stages of infection [19]. In contrast, type I interferons (IFN) can also be induced but are thought

to aid in creating a more permissive environment for bacterial growth. Type I IFNs inhibit IL-1β production, but IL-1β can induce PGE_2 production which inhibits production of type I IFNs, therefore the current model states that a balance between type I IFNs and IL-1β is necessary for adequate containment of infection [18].

Overall to survive in these niches, Mtb must thwart the many defenses of the host immune system as well as scavenge nutrients from immune cells and the acellular core of granulomas. The nutrients critical to Mtb survival, how Mtb manipulates its surroundings to gain access to these nutrients, and how these nutrients are used to synthesize critical virulence factors are described in subsequent sections.

Lipid Utilization in vivo

Mtb was observed to preferentially utilize host lipid as early as the 1950's and this preference is reflected in its genetic repertoire as the Mtb genome encodes for approximately 250 different enzymes involved in the breakdown and biosynthesis of lipids [20, 21]. Transcriptional and functional studies provide further evidence that Mtb uses host-derived lipids *in vivo*. Mtb up-regulates fatty acid and cholesterol metabolic genes during infection [22, 23] and the bacteria have the ability to accumulate exogenous fatty acids during macrophage infection, incorporating them into components of their cell wall [24, 25]. Additionally, Mtb mutants lacking necessary genes for lipid utilization experience growth defects and are attenuated during infection, highlighting the importance of this nutrient in long-term survival of Mtb [26-30].

There are multiple possible routes in which Mtb could obtain lipid nutrients from the host and studies using radiolabeled or fluorescently labeled lipids have shown that Mtb has the ability to import host-derived lipids, including arachidonic acid, free oleic acid, and fatty acids derived from triacylglycerol (TAG), and cholesterol [24, 25, 31, 32]. Inside macrophages the Mtb-containing phagosomes remain fusogenic with endosomes, where the bacteria could access host nutrients through recycling endosomes that fuse with the Mtb-containing vacoule [33-35]. Additionally, Mtb infected macrophages can develop a lipid-loaded phenotype associated with the accumulation of cholesterol, cholesteryl-ester, and triacylglycerol that form lipid droplets in the macrophage which Mtb could potentially have access to [36-38]. Additionally, these lipid droplets also function as sites of eicosanoid biosynthesis as a result of arachidonic acid metabolism; Mtb is capable of importing and metabolizing arachidonic acid, although the effect that this has on the host in unclear [39, 40]. Mtb can also be found in the center of necrotic granulomas, which is an acellular environment consisting of cellular debris [14, 15]. This caseous center contains cholesterol, cholesteryl-ester, and triacylglycerol (Figure 1.1) [41].

While Mtb has been observed to utilize lipids as a carbon source since the 1950's and much has been discovered related to cholesterol and fatty acid metabolic pathways, it was not until recently that studies have begun to uncover the mechanisms by which Mtb imports lipids [20, 42].

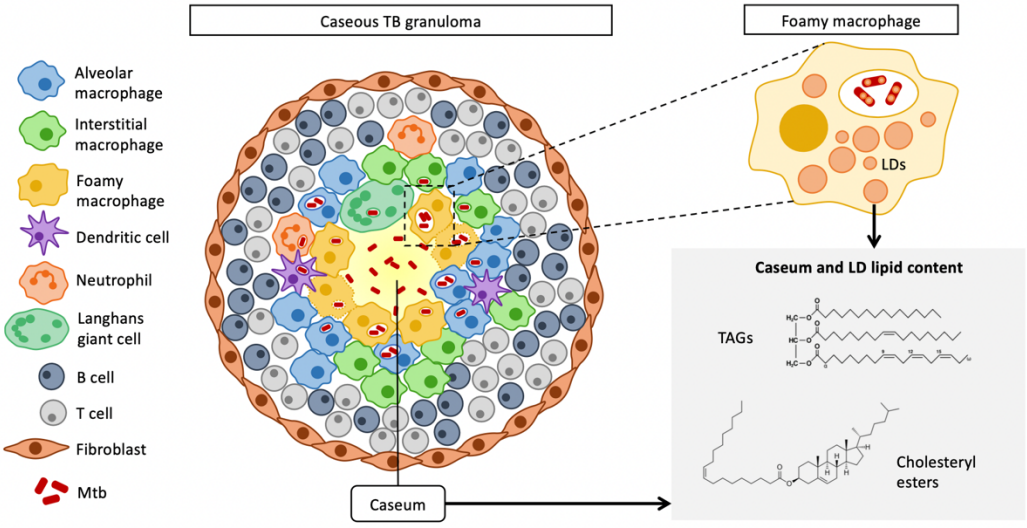

Figure 1.1. Mtb scavenges host lipids during infection. Both cholesteryl-esters and TAGs can be found in the necrotic center of granulomas where Mtb replicate extracellularly and in macrophage lipid droplets located adjacent to Mtb-containing endosomes. Image from [43].

Role of Mce Transporters in Lipid Uptake

To acquire host lipids, Mtb employs transporters that resemble ATP Binding Cassette (ABC) importers. These transporters are encoded by the mammalian cell entry (*mce*) operons; there are four homologous *mce* operons (*mce1-4*) present in the genome of Mtb and each operon encodes two permease-like subunits (*yrbEA* and *yrbEB*) and six Mce genes (*mceA-F*) [21]. The Mce proteins contain Mce domains belonging to the MlaD superfamily and resemble substrate binding proteins [21, 22]. Except for *mce2*, each operon encodes accessory proteins hypothesized to play a structural or regulatory role [21, 23, 24]. Encoded elsewhere in the genome is a putative ATPase termed MceG that is thought to provide energy for translocation via

hydrolysis of ATP, and it is hypothesized that this ATPase associates with all the Mce complexes [25].

Recently, a cyro-EM structure of the Mce1 transporter from *Mycobacterium smegmatis* has been presented depicting the transporter as a complex that spans the entirety of the cell envelope [44]. More specifically, bound to the YrbE permeases which are embedded in the cytoplasmic membrane, the MceA-F proteins form a heterohexameric channel that extends through the pseudo-periplasmic space and across the outer membrane. It is hypothesized that lipid substrates enter the hydrophobic channel formed by MceA-F and are shuttled across the cell envelope to the YrbE permeases. ATP hydrolysis via the ATPase MceG likely causes conformational changes in the permeases which facilitates translocation of the lipids across the cytoplasmic membrane. Although direct evidence for the role of MceG in the function of all Mce transporters is lacking, an MceG mutant strain of Mtb is deficient in its ability to utilize cholesterol suggesting it is required for this process [17, 26]. While structural data is beginning to be available, mechanistic data explaining how these complexes are regulated is severely lacking.

Functionally, these Mce complexes provide nutrients to Mtb through the transport of lipids present in the necrotic center of granulomas or scavenged intracellularly within host immune cells. The substrates specifically transported by Mce1 and Mce4 have been well established to be fatty acids and cholesterol, respectively [17, 23]. Mce1 was recently found to be responsible for the import of fatty acids by our lab; a mutant lacking the *mce1* operon is deficient in its ability to import and metabolize both palmitic and oleic acid [23]. Additionally, Mce4 has been

well established as a cholesterol transporter and strains containing a mutated *mce4* operon are severely deficient in their ability to utilize cholesterol [17]. Mce1 and Mce4 are specific for their respective substrates and do not provide redundant function for one another. Curiously, no substrates have been identified to be imported by the Mce2 and Mce3 complexes and therefore the function of the *mce2* and *mce3* operons remains to be determined.

The mce1 and mce4 transporters are required for survival *in vivo* as mutants lacking genes in the *mce1* or *mce4* operon display growth defects in mice. Mtb lacking *mce1* show a growth defect in mice during the first two weeks of infection while strains lacking *mce4* display a growth defect after 2 weeks of infection [45]. Mutating both *mce1* and *mce4* operons results in a compounded fitness cost for the bacteria during infection [46]. The following chapter will address the necessity of MceG for *mce1* and *mce4* function as well as for full fitness *in vivo*. The growth defects seen in Mtb when Mce1 and Mce4 transporter function is disrupted further highlight the importance of lipid utilization by Mtb, but they also raise the possibility that Mtb has redundant modes of lipid uptake as mutants lacking *Mce1* and *Mce4* are not entirely eliminated by the host [46].

Fate of Host Lipids in Mtb: Beyond Fueling Central Metabolism

Upon uptake, lipids can have multiple fates in Mtb. Intact fatty acids can be incorporated directly into TAG, incorporated into membrane phospholipids, or undergo β-oxidation to fuel central metabolism and energy production. Cholesterol degradation on the other hand, generates 2- and 3-three carbon intermediates that fuel

central metabolism for energy production or fuel lipid synthesis pathways dependent on the 3-carbon intermediate, propionyl-CoA. Importantly, intact fatty acids or partially degraded fatty acids can serve as precursors for lipid biosynthesis, feeding anabolic pathways responsible for the diverse range of virulence lipids that are incorporated into the cell envelope and therefore needed for Mtb to persist in the hostile environment of the host [42].

Although its cell composition appeared to be particularly unique, Mtb was originally placed into the category of gram-positives, but as research progressed it became apparent that its cell wall architecture is much more reminiscent of gram-negatives as it contains both a cytoplasmic membrane and an outer mycomembrane (Figure 1.2). The cytoplasmic membrane of Mtb is a phospholipid bilayer made up mostly of cardiolipin, phosphatidyl inositol, and phosphatidyl ethanolamine [47, 48]. Intercalated within the cytoplasmic membrane and anchored into the inner leaflet are phosphatidylinositol mannosides (PIMs) and their derivatives, lipomannans and lipoarabinomannans (LAM). PIMs are unique to actinomycetes, and their hydrophobic properties likely decrease the fluidity of the cell envelope [49, 50]. The next layers of the Mtb cell envelope consist of peptidoglycan covalently attached to arabinogalactan which in turn is covalently attached to a layer of mycolic acids. This layer of mycolic acids serves as the inner leaflet of the mycomembrane. The outer leaflet of the mycomembrane consists of a variety of free lipid species which include: mycolic acids, mycolic acids containing trehalose, called trehalose monomycolate (TMM) and trehalose dimycolate (TDM), sulfolipids, diacyltrehalose (DAT), polyacyltrehalose (PAT), glycerophopholipids, PIMs, and phthiocerol dimycocerosates (PDIM) [51].

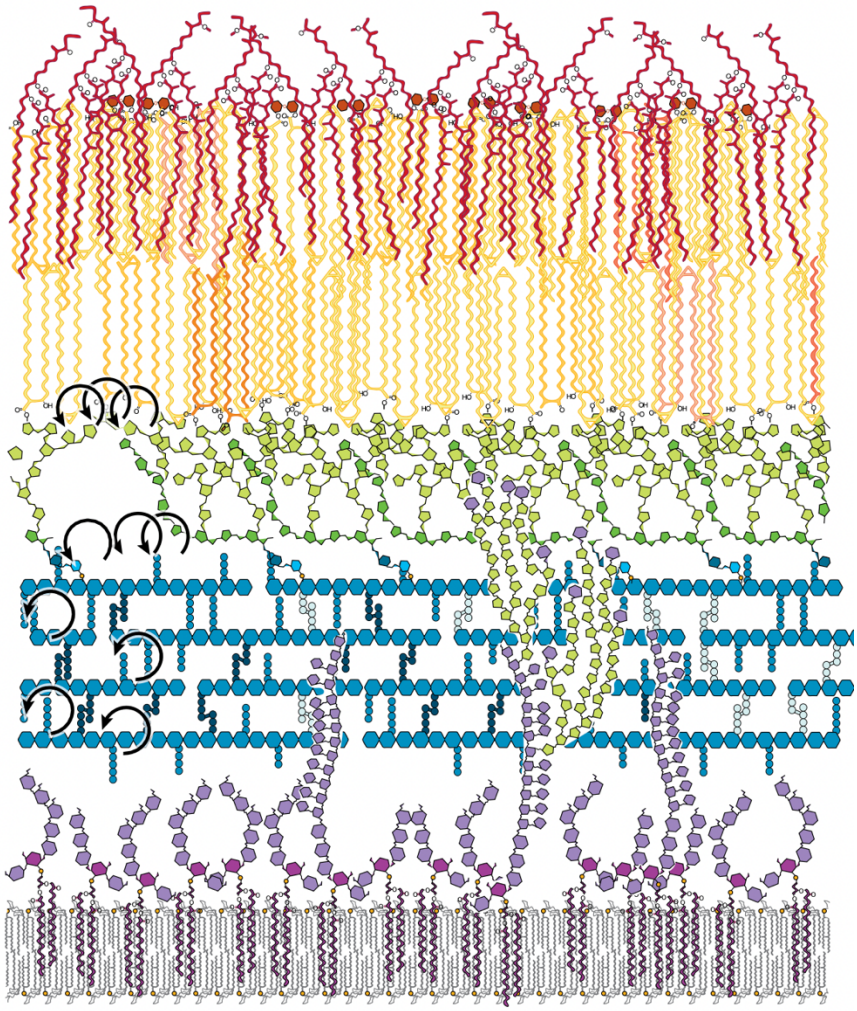

Figure 1.2. Cell envelope of *Mycobacterium tuberculosis*. PIMs and lipomannans (purple) and LAM (green and purple) are embedded into the cytoplasmic membrane. Mtb contains a pseudo-periplasmic space followed by a layer of peptidoglycan (blue) covalently attached to arabinogalactan (green). Mycolic acids (yellow and orange) attached to arabinogalactan form the inner leaflet of the outer membrane. Free mycolic acids, TMM, TDM (dark orange signifies trehalose), and PDIM (red) form the outer leaflet of the outer mycomembrane. Image from [49]

As illustrated, the cell envelope of Mtb contains a diverse range of lipids embedded throughout. While Mtb does have the biosynthetic repertoire to synthesize fatty acids *de novo*, it can also incorporate fatty acids directly into phospholipids destined for the cell membrane or into TAG which functions as a storage molecule. Additionally, fatty acids can be elongated by polyketide synthases to produce polyketide derived lipids, which include PDIM, DAT, PAT, and sulfolipids (SL). Degradation of cholesterol also frees carbon for use in lipid biosynthesis, notably cholesterol breakdown produces propionyl-CoA which is assimilated into polyketide derived lipids as well (Figure 1.3) [42, 51, 52]. Overall, uptake of host lipids is crucial for production of the diverse lipids incorporated into the mycobacterial cell envelope and these lipids serve as important virulence factors for Mtb.

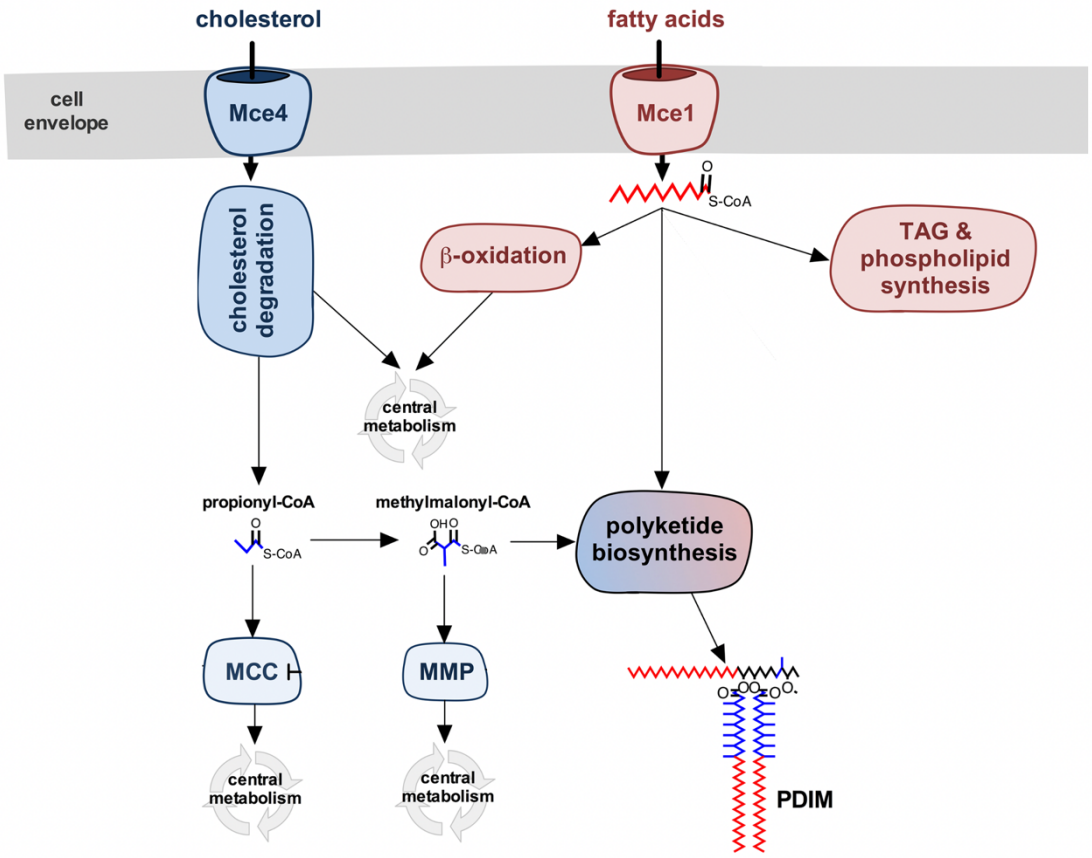

Figure 1.3. Fate of host-derived lipids in Mtb. Cholesterol imported by Mce4 is metabolized producing propionyl-CoA which can enter central metabolism through the methylcitrate cycle (MCC) or be converted to methylmalonyl-CoA and enter the methylmalonyl pathway (MPP). Propionyl-CoA and methylmalonyl-CoA can also be used as precursors for biosynthesis of polyketide derived lipids, including PDIM. Fatty acids imported by Mce1 can also be metabolized providing substrates for central metabolism or they can be used as precursors for synthesis of polyketide lipids, phospholipids, or TAG. Image adapted with permission from [42].

Mtb Lipids as Virulence Factors

Mtb lipids can interact with the host passively via direct contact of the bacteria with host cells or through slight shedding of the lipids in close proximity to host components [53]. Alternatively, lipids can bud off the bacterial envelope in the form of vesicles prior to phagocytosis and while in the phagosome where these bacterial-derived vesicles are thought to be further transported via exocytosis out of the host cell [54, 55]. Bacterial lipids can also be trafficked in the host intracellularly to other compartments and extracellularly via host-derived vesicles where they encounter major histocompatibility complexes (MHC), pattern recognition receptors (PRRs), and can be taken up by other immune cells [54]. Overall, it is thought that these interactions modulate the immune response allowing Mtb to establish and maintain an infection.

At the outset of infection, Mtb lipids will first encounter pattern recognition receptors, such as toll-like receptors (TLR) and C-type lectin receptors, on innate immune cells and once phagocytosed Mtb lipids can further modulate the immune response through interactions with various host components. For example, mannose capped LAM (ManLAM) and some variants of PIMs are recognized by C-type lectin receptors on macrophages which induce phagocytosis [56]. Once in the phagosome, Mtb sheds a lipid named 1-TbAd that acts as an antacid to counter acidification of the compartment, and this lipid also plays a role in preventing fusion of the phagosome with the lysosome [57]. LAM, PIMs, TDM, and SL have also all been implicated in preventing phagosome-lysosome fusion and the presence of TDM is necessary for granuloma formation [53, 58]. In addition, mycobacterial lipids can modulate the

inflammatory response depending on which PRRs they interact with. Induction of inflammatory cytokines, such as TNF-α and IL-12, can occur through recognition of TDM by the C-type lectin receptor Mincle and through recognition of PIMs, LAM, and SL by TLR2 [54, 58-60]. In contrast, recognition of ManLAM by various C-type lectin receptors can have immunosuppressive effects like induction of the anti-inflammatory cytokine IL-10 or suppression of the pro-inflammatory cytokine IL-12 and phenolic glycolipids have been shown to inhibit induction of inflammatory cytokines as well [54, 61]. Overall, lipids in coordination with Mtb secreted proteins facilitate the establishment of an environment where Mtb can avoid being destroyed by the host while still maintaining access to nutrients.

Phthiocerol Dimycocerosates (PDIM) as a Virulence Factor

In addition to the lipids mentioned above, phthiocerol dimycocerosate (PDIM) has been linked to multiple aspects of Mtb pathogenicity, but its exact role has yet to be uncovered. As stated, PDIM is intercalated into the outer leaflet of the mycobacterial outer membrane and contributes to the hydrophobic nature of the cell envelope [62, 63]. PDIM consists of a phthiocerol backbone esterified to two long-chain multimethyl-branched fatty acids, called mycocerosic acids. A 70 kilobase region of the Mtb genome encodes the enzymes needed to synthesize this lipid [64]. Biosynthesis of the phthiocerol backbone occurs via polyketide synthases, ppsA-E, which elongate long-chain fatty acids with malonyl-CoA or methylmalonyl-CoA subunits [65]. Encoded at the end of the PDIM biosynthetic operon is *mas*, the enzyme responsible for biosynthesis of the mycocerosic acids via elongation of fatty acids with

subunits of methylmalonyl-CoA [66]. PapA5, an acyltransferase, is responsible for esterification of phthiocerol with two mycocerosic acids. (Figure 1.4) [67]. The mechanism behind localization of PDIM to the outer membrane remains unclear, but a transporter encoded in the operon, mmpL7, is thought to translocate PDIM across the cytoplasmic membrane and a lipoprotein, LppX, is thought to carry PDIM to the surface [62, 68, 69]. In the host, Mtb consumption of cholesterol causes propionyl-CoA pools to increase and as this metabolite is shunted to PDIM biosynthesis it leads to high mass forms of PDIM as they are longer and contain more methyl groups [70, 71]. Mutations in genes of this operon lead to attenuation *in vivo* during early stages of infection and every clinical isolate recovered from humans contains PDIM, which highlights the importance of this lipid as a virulence factor [72-74].

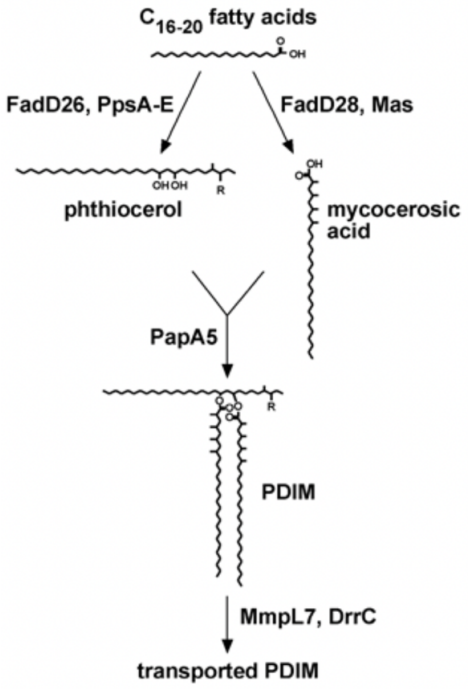

Figure 1.4. Pathway for PDIM biosynthesis in Mtb. Image from [68]

Strains deficient in PDIM biosynthesis or export have been used to elucidate the role PDIM plays in pathogenesis. While it does not appear that PDIM is involved in inhibiting phagosome-lysosome fusion, the lipid is thought to play a role in resisting acidification of the phagosome and preventing induction of nitric oxide (NO) and pro-inflammatory cytokines such TNF-α and IL-6 early in infection [75-78]. It has been proposed that PDIM acts to mask pathogen-associated molecular patterns (PAMPs) on the bacterial surface thereby preventing detection via TLRs and recruitment of NO producing macrophages [79].

Recent studies have provided evidence that PDIM is required for permeabilization of the phagosome in concert with the protein ESAT-6 to allow bacterial PAMPs and the bacteria themselves to gain access to the macrophage cytosol [59, 80, 81]. ESAT-6 is a substrate of the type VII secretion system, ESX-1, that is critical to Mtb pathogenesis as it is proposed to facilitate Mtb escape from the phagosome through its ability to form pores in the phagosomal membrane [16, 82-87]. Upon sensing cytosolic Mtb, macrophages mount a type I IFN response that leads to host cell death, potentially favoring dissemination of the bacteria [83, 85, 88, 89]. PDIM is also required for the same processes, as mutants lacking PDIM are unable to gain access to the cytosol and illicit a type I IFN response leading to host cell death [59, 80, 81]. While one study attests that PDIM is required for ESAT-6 secretion [80], another claims that it is not [81], thereby leaving the question of how PDIM and ESAT-6 may both be linked to phagosomal escape unanswered.

Overall, studies implicate PDIM as a virulence factor that protects Mtb during the initial interaction with the innate immune system and may be important in

phagosomal permeabilization, although the mechanisms underlying these roles remain unclear and the field has not arrived at consensus as to the exact role PDIM plays in Mtb virulence.

Summary

The cell envelope of *M. tuberculosis* is its greatest defense, greatest weapon, and arguably its most distinguishable feature and for Mtb to maintain the unique lipids in its cell envelope, it must scavenge host lipids as a nutrient source. It is known that Mtb utilizes Mce1 and Mce4 transporters to assimilate fatty acids and cholesterol, respectively, but the mechanisms responsible for how these transporters function and how they are regulated remain unknown. Once lipids are taken up by Mtb, they can be catabolized to fuel central metabolism, or they can be used in the biosynthesis of lipids destined for the cell envelope. Lipids of the Mtb cell envelope provide a physical barrier as well as act as significant virulence factors, shaping Mtb's environment in the host. In particular, PDIM is essential to Mtb pathogenesis, but precisely how PDIM influences pathogenesis has been the subject of much debate and further studies are needed to determine its exact role. Overall, bridging the gaps in knowledge regarding host lipid assimilation in Mtb as well as mechanistic details surrounding how Mtb lipids shape the host immune response, would potentially unveil aspects of these pathways that could be exploited by novel therapeutics.

REFERENCES

1. Comas, I., et al., *Out-of-Africa migration and Neolithic coexpansion of Mycobacterium tuberculosis with modern humans.* Nat Genet, 2013. **45**(10): p. 1176-82.

2. *Global tuberculosis report 2022. Geneva: World Health organization; 2022. licence: CC BY-NC-SA 3.0 IGO.*

3. *Global Tuberculosis Report*. 2018, World Health Organization: Geneva.

4. Gagneux, S., *Ecology and evolution of Mycobacterium tuberculosis.* Nat Rev Microbiol, 2018. **16**(4): p. 202-213.

5. Falkinham, J.O., 3rd, *Surrounded by mycobacteria: nontuberculous mycobacteria in the human environment.* J Appl Microbiol, 2009. **107**(2): p. 356-67.

6. Wirth, T., et al., *Origin, spread and demography of the Mycobacterium tuberculosis complex.* PLoS Pathog, 2008. **4**(9): p. e1000160.

7. Comas, I., et al., *Population Genomics of Mycobacterium tuberculosis in Ethiopia Contradicts the Virgin Soil Hypothesis for Human Tuberculosis in Sub-Saharan Africa.* Curr Biol, 2015. **25**(24): p. 3260-6.

8. Brites, D. and S. Gagneux, *The Nature and Evolution of Genomic Diversity in the Mycobacterium tuberculosis Complex.* Adv Exp Med Biol, 2017. **1019**: p. 1-26.

9. Russell, D.G., et al., *Mycobacterium tuberculosis wears what it eats.* Cell Host Microbe, 2010. **8**(1): p. 68-76.

10. Chandra, P., S.J. Grigsby, and J.A. Philips, *Immune evasion and provocation by Mycobacterium tuberculosis.* Nat Rev Microbiol, 2022. **20**(12): p. 750-766.

11. Russell, D.G., *Mycobacterium tuberculosis and the intimate discourse of a chronic infection.* Immunol Rev, 2011. **240**(1): p. 252-68.

12. Ernst, J.D., *The immunological life cycle of tuberculosis.* Nat Rev Immunol, 2012. **12**(8): p. 581-91.

13. Ravesloot-Chavez, M.M., E. Van Dis, and S.A. Stanley, *The Innate Immune Response to Mycobacterium tuberculosis Infection.* Annu Rev Immunol, 2021. **39**: p. 611-637.

14. Hunter, R.L., C. Jagannath, and J.K. Actor, *Pathology of postprimary tuberculosis in humans and mice: contradiction of long-held beliefs.* Tuberculosis (Edinb), 2007. **87**(4): p. 267-78.

15. Martin, C.J., A.F. Carey, and S.M. Fortune, *A bug's life in the granuloma.* Semin Immunopathol, 2016. **38**(2): p. 213-20.

16. Simeone, R., et al., *Phagosomal rupture by Mycobacterium tuberculosis results in toxicity and host cell death.* PLoS Pathog, 2012. **8**(2): p. e1002507.

17. Mayer-Barber, K.D., et al., *Caspase-1 independent IL-1beta production is critical for host resistance to mycobacterium tuberculosis and does not require TLR signaling in vivo.* J Immunol, 2010. **184**(7): p. 3326-30.

18. Mayer-Barber, K.D., et al., *Host-directed therapy of tuberculosis based on interleukin-1 and type I interferon crosstalk.* Nature, 2014. **511**(7507): p. 99-103.

19. Chen, M., et al., *Lipid mediators in innate immunity against tuberculosis: opposing roles of PGE2 and LXA4 in the induction of macrophage death.* J Exp Med, 2008. **205**(12): p. 2791-801.

20. Bloch, H. and W. Segal, *Biochemical differentiation of Mycobacterium tuberculosis grown in vivo and in vitro.* J Bacteriol, 1956. **72**(2): p. 132-41.

21. Cole, S.T., et al., *Deciphering the biology of Mycobacterium tuberculosis from the complete genome sequence.* Nature, 1998. **393**(6685): p. 537-44.

22. Schnappinger, D., et al., *Transcriptional Adaptation of Mycobacterium tuberculosis within Macrophages: Insights into the Phagosomal Environment.* J Exp Med, 2003. **198**(5): p. 693-704.

23. Tailleux, L., et al., *Probing Host Pathogen Cross-Talk by Transcriptional Profiling of Both Mycobacterium tuberculosis and Infected Human Dendritic Cells and Macrophages.* PLOS ONE, 2008. **3**(1): p. e1403.

24. Lee, W., et al., *Intracellular Mycobacterium tuberculosis exploits host-derived fatty acids to limit metabolic stress.* J Biol Chem, 2013. **288**(10): p. 6788-800.

25. Daniel, J., et al., *Mycobacterium tuberculosis uses host triacylglycerol to accumulate lipid droplets and acquires a dormancy-like phenotype in lipid-loaded macrophages.* PLoS Pathog, 2011. **7**(6): p. e1002093.

26. Munoz-Elias, E.J. and J.D. McKinney, *Mycobacterium tuberculosis isocitrate lyases 1 and 2 are jointly required for in vivo growth and virulence.* Nat Med, 2005. **11**(6): p. 638-44.

27. Pandey, A.K. and C.M. Sassetti, *Mycobacterial persistence requires the utilization of host cholesterol.* Proc Natl Acad Sci U S A, 2008. **105**(11): p. 4376-80.

28. McKinney, J.D., et al., *Persistence of Mycobacterium tuberculosis in macrophages and mice requires the glyoxylate shunt enzyme isocitrate lyase.* Nature, 2000. **406**(6797): p. 735-8.

29. Sassetti, C.M. and E.J. Rubin, *Genetic requirements for mycobacterial survival during infection.* 2003. **100**(22): p. 12989-12994.

30. Ehrt, S. and K. Rhee, *Mycobacterium tuberculosis metabolism and host interaction: mysteries and paradoxes.* Curr Top Microbiol Immunol, 2013. **374**: p. 163-88.

31. Akaki, T., et al., *Comparative roles of free fatty acids with reactive nitrogen intermediates and reactive oxygen intermediates in expression of the anti-microbial activity of macrophages against Mycobacterium tuberculosis.* Clin Exp Immunol, 2000. **121**(2): p. 302-10.

32. Nazarova, E.V., et al., *Rv3723/LucA coordinates fatty acid and cholesterol uptake in Mycobacterium tuberculosis.* 2017. **6**.

33. Sturgill-Koszycki, S., U.E. Schaible, and D.G. Russell, *Mycobacterium-containing phagosomes are accessible to early endosomes and reflect a transitional state in normal phagosome biogenesis.* EMBO J, 1996. **15**(24): p. 6960-8.

34. Russell, D.G., J. Dant, and S. Sturgill-Koszycki, *Mycobacterium avium- and Mycobacterium tuberculosis-containing vacuoles are dynamic, fusion-competent vesicles that are accessible to glycosphingolipids from the host cell plasmalemma.* J Immunol, 1996. **156**(12): p. 4764-73.

35. Russell, D.G., et al., *Mycobacterium tuberculosis Wears What It Eats.* Cell Host & Microbe, 2010. **8**(1): p. 68-76.

36. Russell, D.G., et al., *Foamy macrophages and the progression of the human tuberculosis granuloma.* Nat Immunol, 2009. **10**(9): p. 943-8.

37. Peyron, P., et al., *Foamy macrophages from tuberculous patients' granulomas constitute a nutrient-rich reservoir for M. tuberculosis persistence.* PLoS Pathog, 2008. **4**(11): p. e1000204.

38. Guo, Y., et al., *Lipid droplets at a glance.* J Cell Sci, 2009. **122**(Pt 6): p. 749-52.

39. Laval, T., et al., *De novo synthesized polyunsaturated fatty acids operate as both host immunomodulators and nutrients for Mycobacterium tuberculosis.* Elife, 2021. **10**.

40. D'Avila, H., et al., *Mycobacterium bovis bacillus Calmette-Guerin induces TLR2-mediated formation of lipid bodies: intracellular domains for eicosanoid synthesis in vivo.* J Immunol, 2006. **176**(5): p. 3087-97.

41. Kim, M.J., et al., *Caseation of human tuberculosis granulomas correlates with elevated host lipid metabolism.* EMBO Mol Med, 2010. **2**(7): p. 258-74.

42. Wilburn, K.M., R.A. Fieweger, and B.C. VanderVen, *Cholesterol and fatty acids grease the wheels of Mycobacterium tuberculosis pathogenesis.* Pathog Dis, 2018. **76**(2).

43. Laval, T., L. Chaumont, and C. Demangel, *Not too fat to fight: The emerging role of macrophage fatty acid metabolism in immunity to Mycobacterium tuberculosis.* Immunol Rev, 2021. **301**(1): p. 84-97.

44. Chen, J., et al., *Structure of an endogenous mycobacterial MCE lipid transporter.* Res Sq, 2023.

45. Sassetti, C.M. and E.J. Rubin, *Genetic requirements for mycobacterial survival during infection.* Proceedings of the National Academy of Sciences of the United States of America, 2003. **100**(22): p. 12989-12994.

46. Joshi, S.M., et al., *Characterization of mycobacterial virulence genes through genetic interaction mapping.* Proceedings of the National Academy of Sciences, 2006. **103**(31): p. 11760-11765.

47. Goren, M.B., *Mycobacterial lipids: selected topics.* Bacteriol Rev, 1972. **36**(1): p. 33-64.

48. Chiaradia, L., et al., *Dissecting the mycobacterial cell envelope and defining the composition of the native mycomembrane.* Sci Rep, 2017. **7**(1): p. 12807.

49. Dulberger, C.L., E.J. Rubin, and C.C. Boutte, *The mycobacterial cell envelope - a moving target.* Nat Rev Microbiol, 2020. **18**(1): p. 47-59.

50. Bansal-Mutalik, R. and H. Nikaido, *Mycobacterial outer membrane is a lipid bilayer and the inner membrane is unusually rich in diacyl phosphatidylinositol dimannosides.* Proc Natl Acad Sci U S A, 2014. **111**(13): p. 4958-63.

51. Jackson, M., *The mycobacterial cell envelope-lipids.* Cold Spring Harb Perspect Med, 2014. **4**(10).

52. Fieweger, R.A., et al., *MceG stabilizes the Mce1 and Mce4 transporters in Mycobacterium tuberculosis.* J Biol Chem, 2023. **299**(3): p. 102910.

53. Augenstreich, J. and V. Briken, *Host Cell Targets of Released Lipid and Secreted Protein Effectors of Mycobacterium tuberculosis.* Front Cell Infect Microbiol, 2020. **10**: p. 595029.

54. Layre, E., *Trafficking of Mycobacterium tuberculosis Envelope Components and Release Within Extracellular Vesicles: Host-Pathogen Interactions Beyond the Wall.* Front Immunol, 2020. **11**: p. 1230.

55. Prados-Rosales, R., et al., *Mycobacteria release active membrane vesicles that modulate immune responses in a TLR2-dependent manner in mice.* J Clin Invest, 2011. **121**(4): p. 1471-83.

56. Torrelles, J.B., A.K. Azad, and L.S. Schlesinger, *Fine discrimination in the recognition of individual species of phosphatidyl-myo-inositol mannosides from Mycobacterium tuberculosis by C-type lectin pattern recognition receptors.* J Immunol, 2006. **177**(3): p. 1805-16.

57. Buter, J., et al., *Mycobacterium tuberculosis releases an antacid that remodels phagosomes.* Nat Chem Biol, 2019. **15**(9): p. 889-899.

58. Ishikawa, E., et al., *Direct recognition of the mycobacterial glycolipid, trehalose dimycolate, by C-type lectin Mincle.* J Exp Med, 2009. **206**(13): p. 2879-88.

59. Augenstreich, J., et al., *ESX-1 and phthiocerol dimycocerosates of Mycobacterium tuberculosis act in concert to cause phagosomal rupture and host cell apoptosis.* Cell Microbiol, 2017. **19**(7).

60. Dao, D.N., et al., *Mycobacterium tuberculosis lipomannan induces apoptosis and interleukin-12 production in macrophages.* Infect Immun, 2004. **72**(4): p. 2067-74.

61. Reed, M.B., et al., *A glycolipid of hypervirulent tuberculosis strains that inhibits the innate immune response.* Nature, 2004. **431**(7004): p. 84-7.

62. Camacho, L.R., et al., *Analysis of the Phthiocerol Dimycocerosate Locus of Mycobacterium tuberculosis. EVIDENCE THAT THIS LIPID IS INVOLVED IN THE CELL WALL PERMEABILITY BARRIER.* J. Biol. Chem., 2001. **276**(23): p. 19845-19854.

63. Jackson, M., G. Stadthagen, and B. Gicquel, *Long-chain multiple methyl-branched fatty acid-containing lipids of Mycobacterium tuberculosis: biosynthesis, transport, regulation and biological activities.* Tuberculosis (Edinb), 2007. **87**(2): p. 78-86.

64. Onwueme, K.C., et al., *The dimycocerosate ester polyketide virulence factors of mycobacteria.* Prog Lipid Res, 2005. **44**(5): p. 259-302.

65. Azad, A.K., et al., *Gene knockout reveals a novel gene cluster for the synthesis of a class of cell wall lipids unique to pathogenic mycobacteria.* J Biol Chem, 1997. **272**(27): p. 16741-5.

66. Azad, A.K., et al., *Targeted replacement of the mycocerosic acid synthase gene in Mycobacterium bovis BCG produces a mutant that lacks mycosides.* Proc Natl Acad Sci U S A, 1996. **93**(10): p. 4787-92.

67. Touchette, M.H., et al., *Diacyltransferase Activity and Chain Length Specificity of Mycobacterium tuberculosis PapA5 in the Synthesis of Alkyl beta-Diol Lipids.* Biochemistry, 2015. **54**(35): p. 5457-68.

68. Jain, M. and J.S. Cox, *Interaction between polyketide synthase and transporter suggests coupled synthesis and export of virulence lipid in M. tuberculosis.* PLoS Pathog, 2005. **1**(1): p. e2.

69. Sulzenbacher, G., et al., *LppX is a lipoprotein required for the translocation of phthiocerol dimycocerosates to the surface of Mycobacterium tuberculosis.* EMBO J, 2006. **25**(7): p. 1436-44.

70. Jain, M., et al., *Lipidomics reveals control of Mycobacterium tuberculosis virulence lipids via metabolic coupling.* Proceedings of the National Academy of Sciences, 2007. **104**(12): p. 5133-5138.

71. Yang, X., et al., *Cholesterol Metabolism Increases the Metabolic Pool of Propionate in Mycobacterium tuberculosis.* Biochemistry, 2009. **48**(18): p. 3819-3821.

72. Camacho, L.R., et al., *Identification of a virulence gene cluster of Mycobacterium tuberculosis by signature-tagged transposon mutagenesis.* Mol Microbiol, 1999. **34**(2): p. 257-67.

73. Cox, J.S., et al., *Complex lipid determines tissue-specific replication of Mycobacterium tuberculosis in mice.* Nature, 1999. **402**(6757): p. 79-83.

74. Goren, M.B., O. Brokl, and W.B. Schaefer, *Lipids of putative relevance to virulence in Mycobacterium tuberculosis: phthiocerol dimycocerosate and the attenuation indicator lipid.* Infect Immun, 1974. **9**(1): p. 150-8.

75. Rousseau, C., et al., *Production of phthiocerol dimycocerosates protects Mycobacterium tuberculosis from the cidal activity of reactive nitrogen intermediates produced by macrophages and modulates the early immune response to infection.* Cell Microbiol, 2004. **6**(3): p. 277-87.

76. Astarie-Dequeker, C., et al., *Phthiocerol dimycocerosates of M. tuberculosis participate in macrophage invasion by inducing changes in the organization of plasma membrane lipids.* PLoS Pathog, 2009. **5**(2): p. e1000289.

77. Murry, J.P., et al., *Phthiocerol dimycocerosate transport is required for resisting interferon-gamma-independent immunity.* J Infect Dis, 2009. **200**(5): p. 774-82.

78. Kirksey, M.A., et al., *Spontaneous phthiocerol dimycocerosate-deficient variants of Mycobacterium tuberculosis are susceptible to gamma interferon-mediated immunity.* Infect Immun, 2011. **79**(7): p. 2829-38.

79. Cambier, C.J., et al., *Mycobacteria manipulate macrophage recruitment through coordinated use of membrane lipids.* Nature, 2014. **505**(7482): p. 218-22.

80. Barczak, A.K., et al., *Systematic, multiparametric analysis of Mycobacterium tuberculosis intracellular infection offers insight into coordinated virulence.* 2017. **13**(5): p. e1006363.

81. Quigley, J., et al., *The Cell Wall Lipid PDIM Contributes to Phagosomal Escape and Host Cell Exit of Mycobacterium tuberculosis.* mBio, 2017. **8**(2).

82. Abdallah, A.M., et al., *Type VII secretion--mycobacteria show the way.* Nat Rev Microbiol, 2007. **5**(11): p. 883-91.

83. Guinn, K.M., et al., *Individual RD1-region genes are required for export of ESAT-6/CFP-10 and for virulence of Mycobacterium tuberculosis.* Mol Microbiol, 2004. **51**(2): p. 359-70.

84. de Jonge, M.I., et al., *ESAT-6 from Mycobacterium tuberculosis dissociates from its putative chaperone CFP-10 under acidic conditions and exhibits membrane-lysing activity.* J Bacteriol, 2007. **189**(16): p. 6028-34.

85. van der Wel, N., et al., *M. tuberculosis and M. leprae translocate from the phagolysosome to the cytosol in myeloid cells.* Cell, 2007. **129**(7): p. 1287-98.

86. Houben, D., et al., *ESX-1-mediated translocation to the cytosol controls virulence of mycobacteria.* Cell Microbiol, 2012. **14**(8): p. 1287-98.

87. Peng, X., et al., *Characterization of differential pore-forming activities of ESAT-6 proteins from Mycobacterium tuberculosis and Mycobacterium smegmatis.* FEBS Lett, 2016. **590**(4): p. 509-19.

88. Manzanillo, P.S., et al., *Mycobacterium tuberculosis activates the DNA-dependent cytosolic surveillance pathway within macrophages.* Cell Host Microbe, 2012. **11**(5): p. 469-80.

89. Stanley, S.A., et al., *The Type I IFN response to infection with Mycobacterium tuberculosis requires ESX-1-mediated secretion and contributes to pathogenesis.* J Immunol, 2007. **178**(5): p. 3143-52.

CHAPTER 2

MceG Stabilizes the Mce1 and Mce4 Transporters in *Mycobacterium tuberculosis**

*Fieweger RA, Wilburn KM, Montague CR, Roszkowski EK, Kelly CM, Southard TL, Sondermann H, Nazarova EV, VanderVen BC. MceG stabilizes the Mce1 and Mce4 transporters in Mycobacterium tuberculosis. J Biol Chem. 2023 Mar;299(3):102910. doi: 10.1016/j.jbc.2023.102910. Epub 2023 Jan 13. PMID: 36642182; PMCID: PMC9947336.

ABSTRACT

Lipids are important nutrients for *Mycobacterium tuberculosis* (Mtb) to support bacterial survival in mammalian tissues and host cells. Fatty acids and cholesterol are imported across the Mtb cell wall via the dedicated Mce1 and Mce4 transporters, respectively. It is thought that the Mce1 and Mce4 transporters are comprised of subunits that confer substrate specificity and proteins that couple lipid transport to ATP hydrolysis, similar to other bacterial ABC transporters. However, unlike canonical bacterial ABC transporters, Mce1 and Mce4 appear to share a single ATPase, MceG. Previously, it was established that Mce1 and Mce4 are destabilized when key transporter subunits are rendered nonfunctional; therefore, we investigated here the role of MceG in Mce1 and Mce4 protein stability. We determined that key residues in the Walker B domain of MceG are required for the Mce1- and Mce4-mediated transport of fatty acids and cholesterol. Previously it has been established that Mce1 and Mce4 are destabilized and/or degraded when key transporter subunits are rendered nonfunctional, thus we investigated a role for MceG in stabilizing Mce1 and Mce4. Using an unbiased quantitative proteomic approach, we demonstrate that Mce1 and Mce4 proteins are specifically degraded in mutants lacking MceG. Furthermore, bacteria expressing Walker B mutant variants of MceG failed to stabilize Mce1 and Mce4, and we show that deleting MceG impacts the fitness of Mtb in the lungs of mice. Thus, we conclude that MceG represents an enzymatic weakness that can be potentially leveraged to disable and destabilize both the Mce1 and Mce4 transporters in Mtb.

INTRODUCTION

Mtb remains a major global health problem and current estimates indicate that Tuberculosis claimed ~1.4 million lives among HIV-negative individuals and caused ~10 million new infections in the year 2021 alone [1]. A defining feature of Mtb infections is that this bacterium persists in tissues for long durations while promoting the tissue pathology needed for dissemination and transmission between individuals [2]. Thus, understanding how Mtb persists in host cells and or tissues could reveal new weaknesses that can be leveraged in drug development to better combat this pathogen.

The complete nutritional requirements of Mtb *in vivo* remain unknown [3] however, it is established that Mtb imports and metabolizes host-derived lipid nutrients to persist in host cells and tissues [4]. Mtb has evolved specialized transporters that import nutrients across its lipid rich cell wall that prevents diffusion of many macromolecules [5]. Polar nutrients are imported through porin-like channels [5-7] while hydrophobic nutrients such as fatty acids and cholesterol are transported via the Mce1 and Mce4 transporters, respectively [8, 9]. It is thought that Mce1 and Mce4 import substrates across the cell wall and deliver lipids directly to permease complexes embedded in the cytoplasmic membrane [4]. Current models predict that the substrate specific components of the Mce1 and Mce4 transporters (substrate binding proteins and permeases) are encoded in two dedicated operons in the Mtb genome [10]. Unlike most other transporter systems, Mce1 and Mce4 appear to use the shared ATPase, MceG, to power transport activity [8, 9, 11] and it is unclear how MceG coordinates ATP hydrolysis in association with these different transporters. Mce1 and Mce4 also share additional proteins to facilitate substrate import and/or

stabilize the transporter complexes. For example, LucA facilitates cholesterol and fatty acid transport via the Mce1 and Mce4 transporters, and also stabilizes the Mce1 transporter in Mtb [8, 12]. Similarly, the Omam family of proteins facilitate cholesterol transport and stabilize the Mce1 and Mce4 transporter homologs in *M. smegmatis* [13, 14].

Given the growing evidence that proteins shared by Mce1 and Mce4 play a stabilizing role for the transporters, we sought to better understand how MceG facilitates Mce1- and Mce4-mediated transport and to determine if the ATPase activity of MceG could be corrupted in such a way to deactivate both Mce1 and Mce4. By deleting MceG or inactivating key residues in the Walker B motif of the protein, we found that components of the Mce1 and Mce4 transporters were destabilized and degraded. Lastly, we confirm that MceG is required for optimal bacterial fitness in the lungs of mice. Together, these studies establish that the MceG is a novel enzymatic weakness that is necessary for powering and stabilizing two different transporters. It is plausible that chemically inactivating MceG could simultaneously corrupt two important nutrient acquisition pathways that contribute to Mtb pathogenesis.

RESULTS

The ATPase activity of MceG is required for fatty acid and cholesterol utilization.

MceG conserves the canonical motifs needed for ATP binding, hydrolysis, and an ABC transporter family signature motif [15]. Previously it has been established that MceG is necessary for Mce4-mediated cholesterol transport in Mtb [9] and a conserved lysine residue in the Walker A motif of MceG (K66) is required for full virulence of Mtb in mice [11]. Since it was not known if the putative active site residues of MceG are needed for substrate transport, we evaluated if the putative Walker B residues in MceG are indeed required for fatty acid and cholesterol import and metabolism. For this, we deleted *mceG* in Mtb (ΔMceG) by allelic exchange and complemented this strain by expressing wild type MceG or variants of the protein where key Walker B residues have been mutated (D188N or E189Q). The bacteria express these variants of MceG from the native MceG promoter in a chromosomally integrating vector. Relative to wild type or the complemented control, the ΔMceG mutant displayed a ~90% reduction in the rate of ^{14}C-palmitic acid import (Fig 2.1A). Bacteria expressing the MceG Walker B variants displayed a similar reduction in the rate of fatty acid import (Fig. 2.1A). We also measured the metabolic oxidation of ^{14}C-palmitic acid and found that there was an ~85% reduction in the amount of fatty acid oxidized by the ΔMceG mutant relative to wild type and the complemented control. Similarly, expressing the MceG Walker B variants failed to complement the ΔMceG mutant and displayed a similar reduction in levels of fatty acid oxidation (Fig. 2.1B).

MceG is also required for cholesterol import and metabolism. Relative to wild type or the complement control, the ΔMceG mutant had a ~50% reduction in the rate of ^{14}C-cholesterol import. The MceG Walker B variants did not fully complement the mutation and displayed ~25% reduction in the rate of ^{14}C-cholesterol import (Fig. 2.1C). Metabolism of ^{14}C-cholesterol was also decreased in bacteria lacking MceG or in bacteria expressing the MceG Walker B variants. The ΔMceG mutant had a defect (~90% decrease) in the ability to metabolize ^{14}C-cholesterol relative to wild type and the complemented control. The MceG Walker B variants failed to complement the ΔMceG mutant and displayed a similar reduction in the levels of cholesterol metabolism relative to the ΔMceG mutant (Fig. 2.1D).

The hydrophobic nature of the Mtb cell wall and cholesterol likely contribute to the relatively high background levels of ^{14}C-cholesterol binding in the ΔMceG mutant using the cholesterol uptake assay [8, 9, 12]. Thus, the defect in $^{14}CO_2$ release likely better reflects the bacterium's inability to import and metabolize the ^{14}C-cholesterol substrate (Fig 2.1D). Still, we sought to establish that non-specific binding of cholesterol to the bacterial cells accounts for the high background levels of ^{14}C-cholesterol binding in the uptake assay. It was previously reported that sodium azide effectively inhibits Mce4-mediated cholesterol transport in *Rhodococcus jostii* [16]. In Mtb, we found that sodium azide effectively inhibited the metabolic conversion of ^{14}C-cholesterol to ^{14}C-CO_2 (Figure S2.1A) but this treatment did not decrease the relative rate of ^{14}C-cholesterol binding in the ΔMceG cells (Figure S2.1B and S2.1C). Thus, even in the absence of MceG, there are substantial levels of ^{14}C-cholesterol binding to the bacterial cells in this assay. It is unclear if the ^{14}C-cholesterol non-specifically

interacts with the bacterial cell wall lipids or is captured by specific proteins. While this assay has relatively high background levels it is still sensitive enough to detect an uncoupling of transport from bacterial metabolism of 14C-cholesterol. For example, Mtb mutants lacking Mam4B transport cholesterol to wild type levels, but these bacteria are unable to metabolize ^{14}C-cholesterol (8).

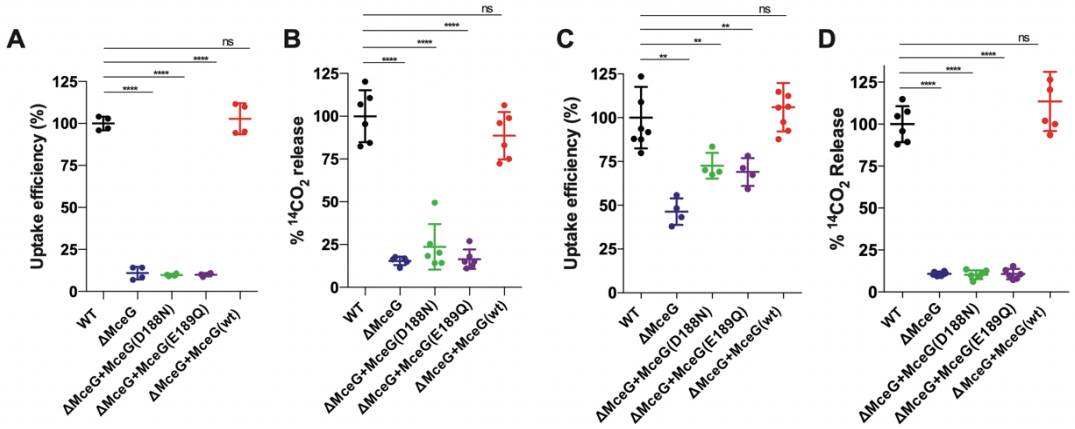

Figure 2.1. The ATPase activity of MceG is required for the utilization of palmitic acid and cholesterol. (A) Whole cell quantification of the rate of palmitic acid import by Mtb cells. (**B**) Metabolic oxidation of palmitic acid to CO_2. (**C**) Whole cell quantification of the rate of cholesterol import by Mtb cells. (**D**) Catabolic release of CO_2 from cholesterol. Data (n ≥ 4) ± SD. Significance was calculated using one-way ANOVA with Dunnett's multiple comparisons test (** $P < 0.01$) ns = not significant. To calculate the Uptake efficiency (%), bacteria were grown in media containing radiolabeled lipids and radioactive counts were measured from the cells over 2 hours; these radioactive counts were used to calculate the rate of lipid uptake which was normalized to wild type for each strain and expressed as a percentage.

The ΔMceG mutant is resistant to fatty acid intoxication.

MceG has been primarily studied in the context of cholesterol import. Therefore, we sought to better characterize the role of MceG in the Mce1-mediated import of fatty acids. Free fatty acids are toxic and prevent the growth of Mtb in liquid culture, and this intoxication is mitigated by including albumin in the media during routine

culturing [17]. While the mechanism of fatty acid intoxication is unclear, we leveraged this intoxication phenotype as an indicator of fatty acid import. As expected, Mtb lacking the Mce1 fatty acid transporter was resistant to fatty acid intoxication in the absence of albumin while wild type Mtb displayed poor growth in this assay (Figure 2.2A). Similarly, Mtb lacking LucA, a protein that facilitates Mce1-mediated import of fatty acids, displayed a resistant phenotype in this growth assay (Figure 2.2A). Mtb lacking MceG was resistant to fatty acid intoxication, while complementation restored the fatty acid intoxication phenotype (Figure 2.2B). These observations further confirm that MceG is required for fatty acid import, and fatty acids are toxic following import into the bacterial cell via the Mcel transporter.

Fatty acid import in macrophages is mediated by MceG.

Next, we assessed the role of MceG in fatty acid uptake during macrophage infection by quantifying bacterial assimilation of fluorescent palmitate (Bodipy-C16). In these experiments, Mtb was engineered to constitutively express mCherry and was used to infect murine macrophages. To track bacterial assimilation of Bodipy-C16 during infection in the macrophages we pulse labeled the infected cells with the dye labeled lipid. Folllowing the pulse label, the bacteria we isolated from macrophages and analyzed by imaging and flow cytometry as described [8]. Bodipy-C16 labeled, intra-bacterial lipid inclusions were visualized in the wild type and complemented strains. In contrast, bacteria lacking MceG produced little to no Bodipy-C16 lipid inclusions (Figure 2.2A). Incorporation of Bodipy-C16 by intracellular Mtb was also quantified by flow cytometry revealing that, relative to wild type and the

complemented strain, we observed an ~85% reduction in the amount of Bodipy-C16 assimilated by bacterial cells lacking MceG (Figure 2.2D). These observations illustrate the essential role that MceG plays in importing fatty acids during macrophage infection.

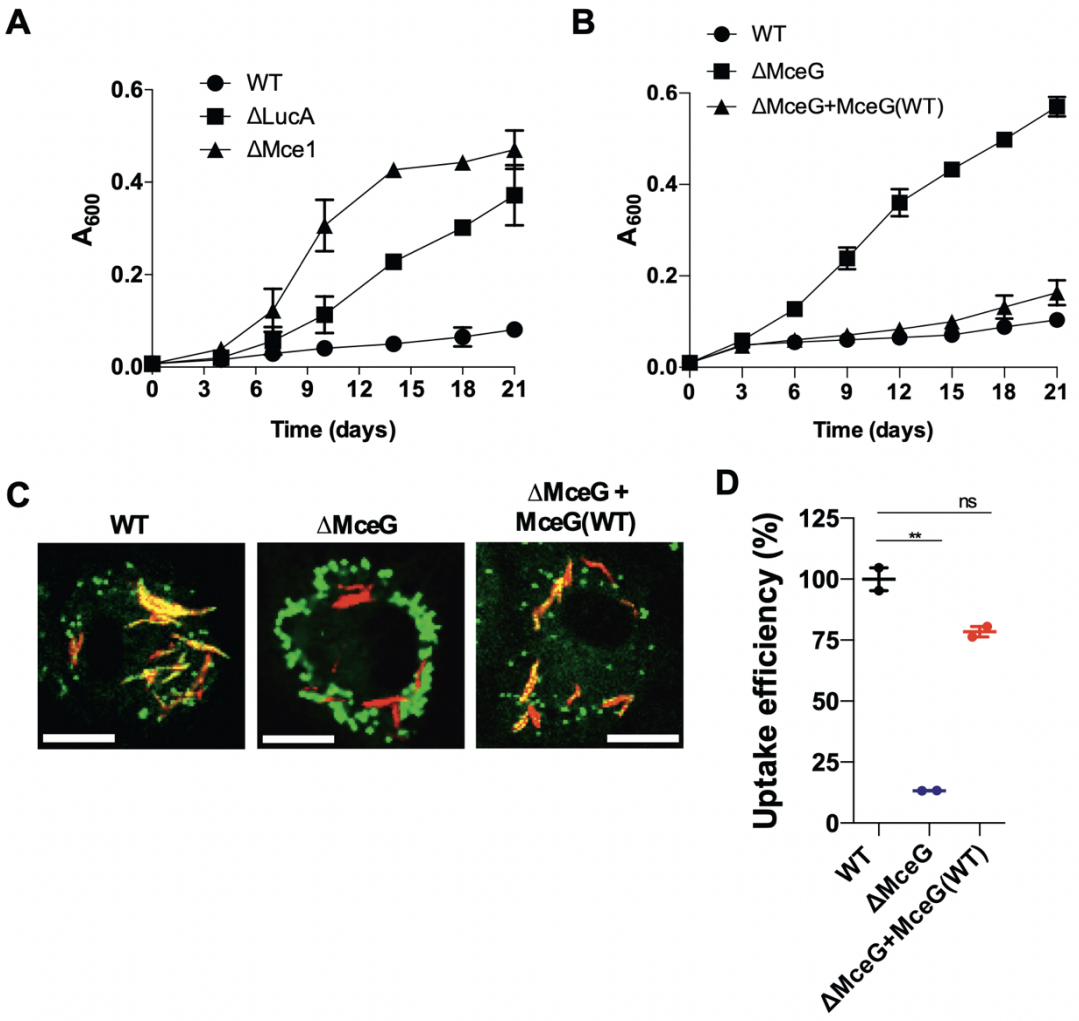

Figure 2.2. MceG is required for fatty acid intoxication and for importing fatty acids during infection in macrophages. (**A**) Inhibition of Mtb growth in minimal media containing 25 μM palmitate (C16) occurs when the bacteria express a functional Mce1 transporter. (**B**) The growth of Mtb lacking MceG is not inhibited in minimal media containing 25 μM palmitate (C16) without albumin. (**C**) Confocal microscopy analysis reveals that Bodipy-C16 does not accumulate in ΔMceG mutant as cytosolic lipid inclusions. Representative confocal images of infected macrophages (red = mCherry Mtb, green = Bodipy-C16). Scale bar 10.0 μm. (**D**) Flow cytometry-

based quantification of Bodipy-C16 incorporation by Mtb isolated from pulse-labeled macrophages. Growth data (n = 4) ± SEM. Bodipy-C16 incorporation was quantified from 10,000 bacteria in each experiment by flow cytometry (n = 2) ± SD. Significance was calculated using one-way ANOVA with Dunnett's multiple comparisons test (** $P < 0.01$) ns = not significant.

Analysis of protein abundance in the ΔMceG mutant.

The Mce1 and Mce4 transporters are destabilized when Omam or LucA subunits are deleted. Thus, it is conceivable that Mce1 and Mce4 could also be destabilized in the ΔMceG mutant. To quantify protein turnover in Mtb lacking MceG, we employed an unbiased proteomic approach. For this, replicate cultures of *Mtb* (wild type n=5, ΔMceG n=6, and complement n=4) were grown to mid-log phase and lysed by sonication to generate SDS solubilized whole cell lysates (WCL). WCL's from each biological replicate were processed for tandem mass tag (TMT) labeling and protease digestion prior LC-MS/MS analysis. In total, this analysis identified 2,429 proteins with a minimum of two unique peptides in each sample. In our analysis we applied a cut-off of $\log_2$(fold change), either more- or less-abundant, with a *P*-value <0.00001 in the ΔMceG samples relative to wild type or the complemented strain (Fig 2.3A). Focusing on proteins common in both of these comparisons, we identified 18 underrepresented proteins in the ΔMceG samples. These were predominantly subunits of Mce transporters, including 8 Mce1 proteins and 5 Mce4 proteins (Figure 2.3B), supporting the idea that MceG stabilizes Mce transporters in Mtb. Recently, a cryo-EM structure of the *M. smegmatis* Mce1 transporter was reported. Our proteomic approach identified homologs for all of the core Mce1 proteins in Mtb including Rv2536/LucB [18]. Importantly, Rv2536/LucB was previously not associated with the

Mce1 transporter. Conversely, one overrepresented protein, Rv1999c, was detected in the ΔMceG mutant relative to the wild type and complement strains (Figure 2.3A). Rv1999c is a putative integral membrane transporter of unknown function and may perhaps play a compensatory transport function in the absence of MceG, Mce1, and Mce4.

Analysis of the bacterial WCL's by immunoblotting confirmed that the putative Mce1 substrate binding proteins (Mce1A, Mce1D, and Mce1E) are degraded or less abundant in the ΔMceG mutant and in Mtb expressing the variants of MceG (D188N or E189Q) (Figure 2.4B). To test if MceG and MceG ATPase activity is required to stabilize Mce proteins, bacterial cells were treated with chloramphenicol to prevent new protein synthesis and protein decay of select Mce proteins was evaluated by Western blot. We found that the levels of Mce1D and the MceG (D188N) variant were reduced following chloramphenicol treatment (Figure S2.2). Importantly, cells expressing wild type MceG, the Mce1D and MceG (D188N) variant protein remain stable and detectable in the presence of chloramphenicol treatment (Figure S2.2). Mce protein turnover in the absence of any detectable gene expression differences is considered a property of Mce transporter destabilization in Mtb [8, 13]. Quantification of *mceG*, *mce1* and *mce4* transcript levels using qPCR confirmed that gene expression of these genes and operons is equivalent between all strains, and depletion of Mce1 and Mce4 proteins is not due to a reduction in gene expression (Figure 2.4C). These data provide evidence that MceG, and, more specifically residues in the Walker B motif of MceG plays a role in stabilizing components of the Mce1 and Mce4 transporter complexes. While protein concentration in cells is a product of synthesis

and degradation, these data suggest that Mce proteins are subject to decay when MceG is deleted or lacks critical ATPase active site residues.

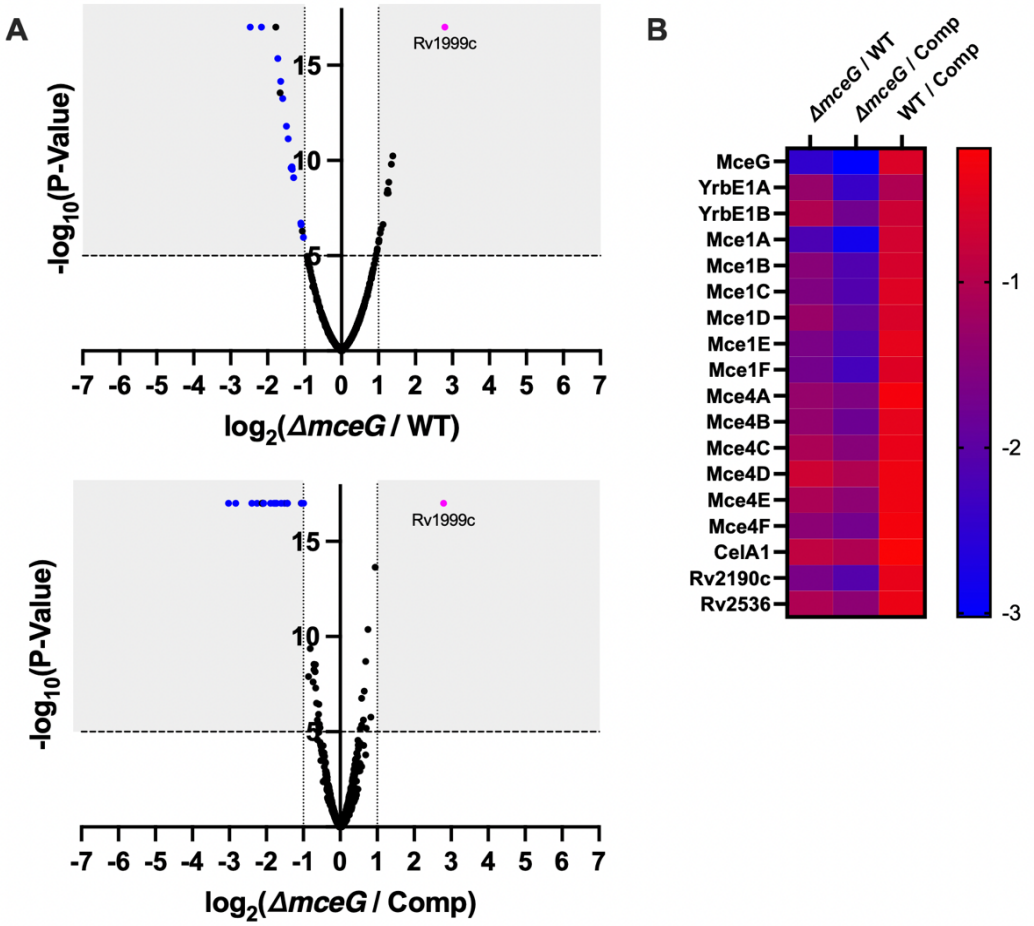

Figure 2.3. Relative protein abundance in the ΔMceG mutant. (**A**) Abundance ratios were determined for 2,429 proteins identified in proteomic analysis with coverage of two or more unique peptides coverage identified in the ΔMceG strain relative to wild type (top), or the complemented strain (bottom). Shaded area indicates proteins with two-fold differences, $P < 0.00001$. Blue dots indicate Mce-associated proteins in the shaded regions of both plots, pink dot indicates Rv1999c. **(B)** Heat map of proteins underrepresented in the ΔMceG strain relative to wild type or the complemented strain with of two-fold or greater differences and a $P < 0.00001$). Scale indicates $\log_2$(fold change).

MceG exhibits ATPase activity.

Importantly, the enzymatic activity of MceG has not yet been experimentally demonstrated. Therefore, we sought to detect ATPase activity from MceG. To do this, wild type MceG and a version of MceG containing a mutated Walker B motif (D188N) were each fused to an N-terminal His-SUMO tag to enhance solubility and purification from *E. coli*. The recombinant proteins were purified to homogeneity and analyzed for ATP hydrolysis activity. The effective activity for wild type MceG was 0.198 +/- 0.007 P_i min^{-1} (Figure S2.3). The MceG (D188N) variant exhibited background ATP hydrolysis activity (0.096 +/- 0.002 P_i min^{-1}) which is likely due to partial inactivation of the enzyme or a contaminating ATPase carried over from the purification process (Figure S2.3). This low but detectable ATPase activity with wild type MceG likely reflects a requirement for additional protein components of the Mce transporters for full MceG ATPase activity similar to what has been observed with the related *E. coli* Mla transporter [19, 20].

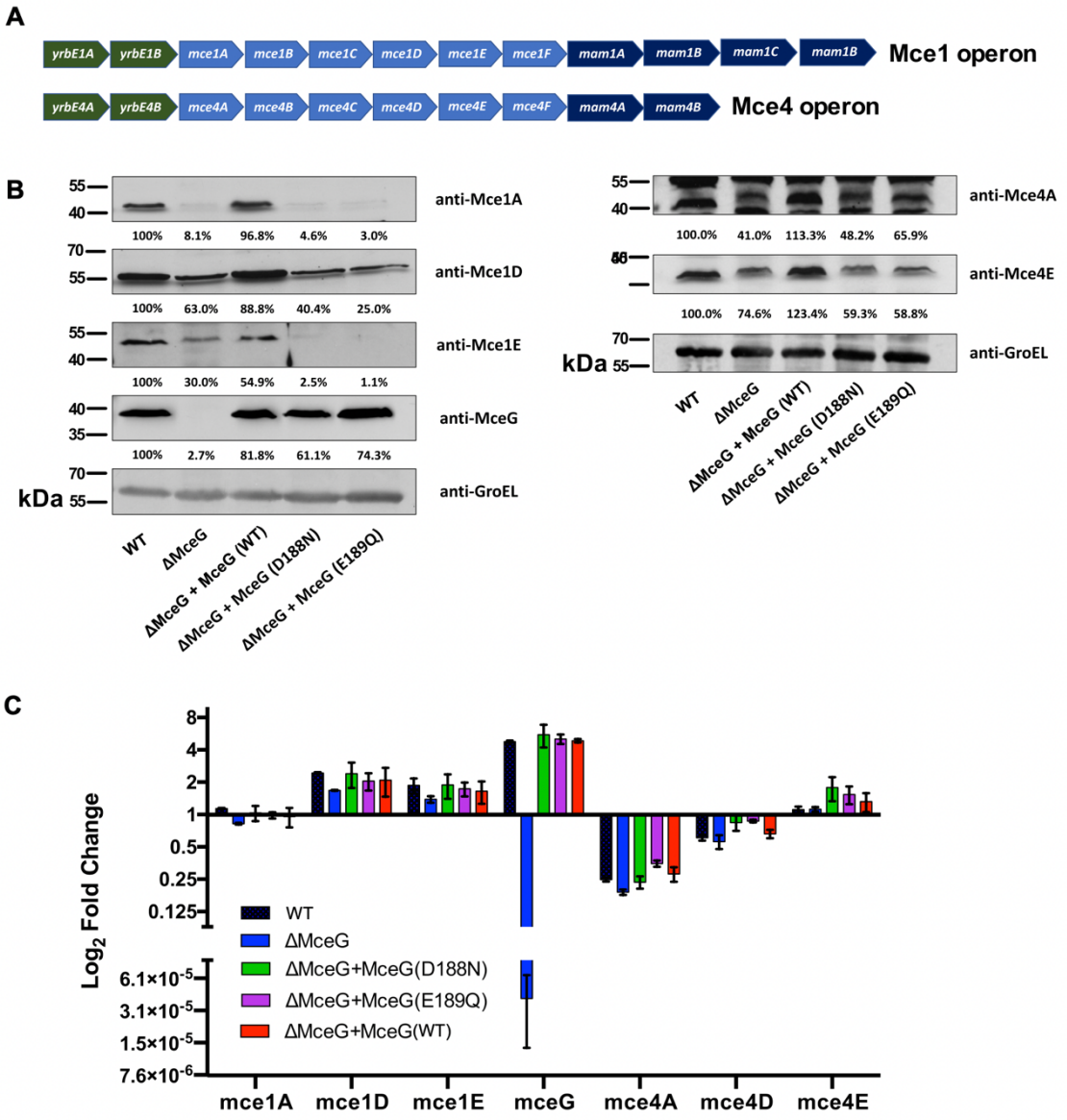

Figure 2.4. MceG ATPase activity is required to stabilize the Mce1 transporter complex. (**A**) Genetic organization of the Mce1 and Mce4 operons. **(B)** Mtb whole cell lysates probed with antibodies specific to protein of the Mce transporters and GroEL2 as the loading control. Western blots depicted are representative images of two independent replicates. Densitometry was performed with each western blot and all values were normalized to those of the corresponding loading control. Ratios of the proteins levels of an individual lysate compared to the corresponding wild type lysate are expressed as percentages inset below each blot. (**C**) qPCR quantification of RNA transcripts from the Mce1 and Mce4 operons. Transcript levels were normalized to the housekeeping gene, *sigA*.

MceG is required for full fitness in murine lung tissue.

The *in vivo* fitness of an MceG mutant has only been reported from mice using an intravenous, competitive infection assay [11]. Mtb mutants lacking LucA are unable to import both cholesterol and fatty acids, and have a colonization defect in the lungs of mice [8]. Therefore, we characterized the MceG mutant using the same infection model and found that the ΔMceG mutant grew poorly during the first 2-3 weeks in mice resulting in a ~0.5-1.0 $\log_{10}$ reduction in colony forming units (CFUs) across the remainder of the infection (Fig 2.5A). The decrease in bacterial CFUs correlates with a reduction in the levels of inflammation in the lungs (Fig 2.5B).

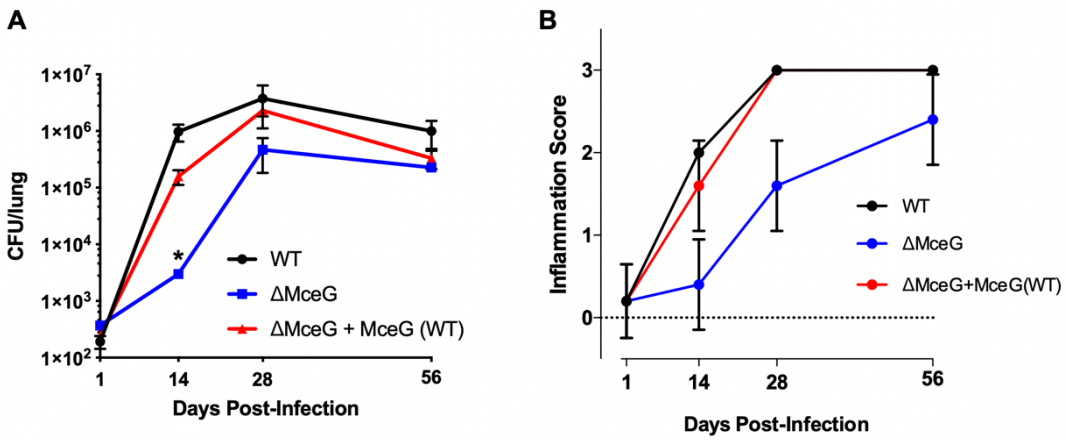

Figure 2.5. MceG is required for Mtb survival *in vivo*. (**A-D**) BALB/c mice were infected by intranasal inoculation using similar numbers of bacteria. (**A**) Colony forming units of wild type, ΔMceG, and ΔMceG+MceG(wild type) bacteria from the lungs of mice individually plotted. (**B**) Histopathology as scored by a pathologist in a blinded manner. Score numbers represent the extent of inflammatory lesions: 0, no lesions; 1, mild inflammation; 2, moderate inflammation; 3, marked inflammation. Data represent two or more independent experiments. Data are means ± SEM. Significance was calculated using Mann-Whitney test (* $P < 0.05$).

DISCUSSION

The Mce1 and Mce4 transporters appear to be comprised of core substrate specific proteins but also share specific subunits such as MceG, LucA, and Omam proteins [8, 12, 13]. This is a highly unusual arrangement for a transporter family, and how all of these proteins coordinate with the different Mce transporters remains unknown. Transporter ATPase subunits do mechanical work by undergoing conformational changes following ATP hydrolysis by transferring energy to coupling helices of permease proteins during substrate translocation [21]. Each of the four Mce transporters in Mtb are thought to consist of two integral membrane permease proteins, termed YrbE1-4A and YrbE1-4B. All eight of these putative permease proteins have similar predicted transmembrane topologies with a homologous, 47 amino acid cytosolic loop containing an EExDA motif which is a strong candidate for a shared MceG binding site analogous to a coupling helix [10]. While MceG may also stabilize Mce2 and Mce3 in Mtb, we did not reliably detect depletion of these proteins; this is partly because of their limited expression under the growth condition used [22, 23].

Low levels of MceG ATPase activity were detected using recombinant MceG alone, and full ATPase activity will likely require purifying MceG in a complex with additional Mce transporter proteins. The MceG Walker A domain is thought to coordinate ATP binding via hydrogen bonding with β-phosphate, and the Walker B domain could provide the carboxylate residue needed to coordinate Mg^{2+} for ATP hydrolysis [24]. We focused on mutating the catalytic residues in the Walker B motif of MceG because chaperone ATPases lacking these residues can bind ATP but cannot

hydrolyze it [25]. The Walker B mutations in MceG were sufficient to destabilize Mce1 and Mce4 suggesting ATP hydrolysis is also needed to maintain Mce1 and Mce4 stability and/or function. A recent report describes a stability-based mechanism thought to regulate the *E. coli* Mla transporter which facilitates movement of phospholipids across the periplasm and utilizes an ABC ATPase, MlaF, to energize this process [26]. In this model, a soluble STAS-domain containing protein, MlaB, is proposed to regulate the Mla transporter by stabilizing the MlaF dimer, either by preventing its degradation or by increasing affinity of MlaF for the transporter [19]. It is possible that additional factors such as LucA or the Omam proteins may be required to facilitate the binding of MceG to the Mce transporters, leading to stabilization of the Mce transporters.

Free fatty acids are known to intoxicate bacteria by disrupting membrane functions [27, 28] or inducing lipid peroxidation reactions in cells [29]. It is well established that Mtb can be intoxicated by fatty acids in liquid media that lacks carrier proteins such as albumin [17, 30, 31]. Complexing free fatty acids to albumin in media formulations likely limits Mtb's ability to import and/or metabolize these substrates. While the mechanism of fatty acid intoxication in Mtb remains unclear, this intoxication phenotype correlates with Mtb's ability to import fatty acids suggesting an intoxication process that occurs following delivery of the fatty acids into the Mtb cell.

In our proteomic analysis, the Mce1 and Mce4 transporter proteins are the most underrepresented proteins in ΔMceG mutant, with the exception of three proteins (Rv2536, Rv2190/RipC and Rv0062/CelA1) (Fig 3B). The function of Rv2536 is unknown, but peptides from this putative membrane protein bind mammalian cell

surfaces with high affinity [32], a property similar to other Mce proteins [33]. Rv2190/RipC is a member of the of NlpC/P60 family of proteins that hydrolyze proteins, peptidoglycan fragments, and catalyze acyl transfer reactions [34]. *In vitro*, Rv2190/RipC has weak but detectable peptidoglycan hydrolase activity which is stimulated by binding to the cell division protein, FtsX [35]. The role of Rv2190/RipC in Mtb cell division is unclear but mutants lacking Rv2190/RipC are attenuated in the TB mouse model and have altered cell morphology associated with cell wall integrity defects [36]. While we did not observe any obvious colony morphology differences in the ΔMceG mutant, we cannot exclude that some of the *in vivo* phenotype of ΔMceG observed could also reflect depletion of Rv2190/RipC. Our future work will determine whether Rv2190/RipC is involved in the turnover of the Mce1 and Mce4 transporters. Lastly, Rv0062/CelA1 is a putative secretory protein with cellulase activity [37] that is capable of degrading the types of extracellular carbohydrates produced by Mtb [38]. These results suggest that there is a dynamic remodeling of the Mtb cell wall to accommodate Mce transporter function or to maintain the cell wall in the absence of these transport complexes.

Several practical challenges exist that make targeting nutrient utilization in Mtb for drug development difficult. Mtb can simultaneously import and metabolize various nutrients and seemingly lacks a canonical catabolite repression system [39]. Mtb also colonizes various tissues and host cells during infection and is therefore thought to be exposed to a variety of different nutrient types in its natural environment [3, 40, 41]. Additionally, the lipid catabolic pathways in Mtb are likely highly redundant and true rate-limiting bottlenecks in these pathways are only beginning to be understood [42].

However within macrophages, Mtb encounters some nutritional constraints that impose a preference for the bacteria to metabolize fatty acids and cholesterol [43]. Therefore, chemically corrupting cholesterol and fatty acid import in Mtb could negatively impact bacterial fitness during infection in macrophages or lipid-rich environments of necrotic granulomas. This work suggests that effective chemical inhibitors of MceG would be predicted to block Mtb's ability to utilize multiple key lipid nutrients simultaneously while negatively impacting bacterial fitness, which may enhance antibiotic treatment options for TB.

EXPERIMENTAL PROCEDURES

Strains and growth conditions

The *E coli* strains Top10 (Invitrogen) and T7 Express (New England Biolabs) were used for molecular cloning. *E. coli* strains were grown in LB medium and transformants were selected on LB plates containing kanamycin (25 μg ml^{-1}), ampicillin (100 μg ml^{-1}) or hygromycin (100 μg ml^{-1}). For protein expression, the *E coli* strain BL21 (DE3) (Stratagene), was used and strains were grown in LB medium or Terrific Broth media containing antibiotics. Mtb Erdman strains were cultivated in 7H9 medium (BD Biosciences) containing OADC supplement (BD Biosciences) unless otherwise noted. 7H12 base medium was used as previously described [43] and supplemented with cholesterol (100 μM), fatty acids (100 μM), or sodium acetate (0.1%). Stock solutions (1000x) of lipid substrates were solubilized in a (1:1 v/v) solution of tyloxapol (Sigma) and ethanol and heated to 65°C prior to adding into media to the final concentration of tyloxapol at 0.05%. The Δ*mce1* and Δ*lucA* mutant strains were generated in [8]. To create the Δ*nceG* mutant strain, the internal region of the *rv0655* open reading frame (111 bp -499 bp) was replaced with a hygromycin cassette via allelic exchange and confirmed with sequencing [44]. For fatty acid toxicity studies Mtb strains were cultured to mid-log phase in 7H9 OADC + 0.05% tyloxapol, and then inoculated at an OD_{600} of 0.005 into 10 ml of 7H12 media lacking casitone and supplemented with 25 μM palmitate. Cultures were incubated at 37˚C for 21 days and an OD_{600} measurement was taken every 3-4 days over the course of the incubation period.

Protein expression and purification

To express recombinant MceG, a plasmid containing a truncated version of wild type or mutant MceG fused at the N-terminus to a His_6-SUMO tag were transformed into *E. coli* BL21 (DE3) cells. To generate MceG point mutants, site-directed mutagenesis was performed using the QuickChange method (Agilent). For protein expression, these strains were cultured in 18.0 liters of Terrific Broth medium containing kanamycin (50 μg ml^{-1}) to an OD_{600} of 0.6 at 37˚C. The temperature was then lowered to 18˚C and 0.5 mM IPTG (Sigma) was added to induce gene expression. Cultures were incubated for 16 hours at 18˚C and shaking at 220 rpm. Cells were harvested by centrifugation and sonicated in Buffer A (25 mM Tris HCl, pH 8.5, 500 mM NaCl, 20 mM imidazole). Centrifugation was used to remove debris and the His-tagged proteins were affinity purified using Ni-NTA resin. Protein was eluted off the resin with Buffer B (25 mM Tris HCl, pH 8.5, 500 mM NaCl, 500 mM imidazole). A HiPrep 26/10 Desalting column (GE Life Sciences) was used to buffer exchange the protein into gel filtration buffer (25 mM Tris HCl, pH 7.5, 150 mM NaCl), and it was further purified using an S200 size exclusion chromatography column (GE). Purified protein from peak fractions was concentrated to 10 mg ml^{-1} and stored at -80 ˚C. Protein purity was assessed via SDS-PAGE and Coomassie staining.

ATPase assay

ATPase activity of recombinant wild type or mutant MceG was measured using the Enzcheck Phosphate Assay kit (Invitrogen). A reaction mixture was made following the kit instructions and scaled to reaction volume of 200 µL. The reaction mixture was added to a 96-well plate along with recombinant wild type or mutant

MceG at concentrations of 2.5, 5, 12.5, and 25 μM. Following the addition of 0.5 mM ATP, inorganic phosphate accumulation was assessed over time through measurement of the absorbance at 360 nm using an Envision plate reader (Perkin Elmer).

Lipid uptake assays

Lipid uptake was quantified as described [8] with slight modifications. Briefly, Mtb was cultured in vented T-25 tissue culture flasks with 7H9 base media supplemented with 0.5% BSA Fraction V, 0.2% dextrose, 0.01% glycerol, and 0.05% tyloxapol for 5 days. At the mid log phase of growth, the bacteria were harvested and the cell density was adjusted to an OD_{600} of 0.7 in 7.0 ml of spent medium and were incubated with 1 μCi of [^{14}C(U)]-palmitate (Perkin Elmer) or [4-^{14}C] cholesterol (Perkin Elmer) at 37˚C for 2 hours. Bacterial samples (1.5 ml) were removed at 5, 30, 60, and 120-minute time points and washed three in 1 ml of ice-cold wash buffer (0.1% Fatty acid free-BSA and 0.1% Triton X-100 in PBS), fixed in 0.2 ml of 4% PFA for 1 hr. The total amount of radioactive label associated with the fixed pellet was quantified by scintillation counting. The radioactive signal was normalized to the relative levels of bacterial density at OD_{600} for the bacterial cultures before addition of radioactive label. The uptake rate was calculated by applying linear regression to the normalized radioactive counts over time, and uptake efficiency was expressed as a ratio of uptake rate for each strain relative to the wild type control. The rate of lipid uptake calculated for each strain was then normalized to wild type in order to express the rate as uptake efficiency (%). For sodium azide experiments, flasks were inoculated with sodium azide at a final concentration of 60mM and incubated at room temperature for 10 minutes before radiolabel was added.

Radiorespirometry assays

Lipid oxidation was monitored by quantifying the release of $^{14}CO_2$ from [4-^{14}C]-cholesterol or [^{14}C(U)]-palmitate by radiorespirometry. Mtb cultures were pre-grown in 7H9 base media supplemented with 0.5% BSA Fraction V, 0.2% dextrose, 0.01% glycerol, and 0.05% tyloxapol for 5 days. At the mid log phase of growth, the density of the bacterial cells was adjusted to an OD_{600} of 0.7 in 5 ml of spent medium supplemented with 1.0 μCi of radiolabeled substrates in vented standing T-25 tissue culture flasks placed in a sealed air-tight vessel with an open vial containing 0.5 ml 1.0 M NaOH at 37°C. After 5 hr, the NaOH vial was recovered, neutralized with 0.5 ml 1.0 M HCl, and the amount of base soluble $Na_2{}^{14}CO_3$ was quantified by scintillation counting. Radioactive counts were normalized to the relative levels of bacterial growth by determining the OD_{600} for the bacterial cultures obtained at the 5 hr timepoint. The % CO2 release was expressed as a ratio of normalized radioactive signal for each strain relative to the wild-type control as described [8].

Macrophage isolation and fluorescent fatty acid import assay

Macrophages were derived from the bone marrow from femurs of BALB/c mice (Jackson), 6-8 weeks of age [45]. The bone-marrow-derived macrophages were seeded into T-150 tissue culture flasks (3×10^7 cells per flask) and infected with Mtb at a MOI of 4:1. After 3 days of infection, Bodipy-16 (Thermo Scientific) to a final concentration 8 μM pre-conjugated to de-fatted 1% BSA was added to the cells for 1-hr pulse and then chased with cell media for another hour. The infected macrophages were scraped into 15 ml of homogenization buffer (250 mM sucrose, 0.5 mM EGTA, 20 mM HEPES,. 05% gelatin, pH 7.0) and pelleted by centrifugation at 514xG (1500

rpm, Beckman Allegra 6KR centrifuge, GH-3.8 rotor), followed by cell lysis by 70 passages through a 25-gauge needle. 5 ml of cell lysate was centrifuged at 146xG (800 rpm) for 10 min, supernatant (suspensions of phagosomes) was retained and treated with 0.1% Tween-80 at 4°C for 15 min to lyse Mtb containing vacuoles. Isolated bacteria were washed once in PBS + 0.05% tyloxapol and fixed in 4% PFA. Flow cytometry data were collected on BD FACS LSR II and analyzed using FlowJo (Tree Star, Inc).

Microscopy and image analysis of lipid inclusions

Monolayers of macrophages infected at an MOI of 3:1 in 8-well glass bottom μ-Slides (Ibidi) were pulsed with 8 μM Bodipy-C16 (Thermo Scientific) complexed to fatty acid free BSA as described [8, 12, 46]. Following the pulse labeling period, the cells were chased in fresh media without label for 1 hour. The infected macrophages were imaged by confocal microscopy as described [47].

Quantitative LC-MS/MS proteomics

M. tuberculosis cultures were cultured in 50 ml of 7H9 OADC + 0.05% tyloxapol standing for five days. Bacteria were suspended in 1x PBS containing 1% SDS + protease inhibitors and lysed via sonication on ice. Samples were centrifuged for 10 min at 15,000 RPM. The supernatant was filtered, then submitted to Cornell Proteomics and Metabolomics Facility. Protein concentration for each sample was determined by running on a precast NOVEX 10% Bis-Tris mini-gel (Invitrogen, Carlsbad, CA) with serial amounts of *E. coli* lysates (2.5, 5, 10, 15 μg/lane) serving as a standard curve. The SDS gel was visualized with colloidal Coomassie blue stain

(Invitrogen), imaged by ChemiDoc (BioRad) followed by quantification using Image Lab 6.1 (Bio-Rad).

Proteins were digested and labeled according to Thermo Scientific's TMTpro Mass Tagging Kits and Reagents protocol (Lot number: VL313890) with slight modifications [48-51]. A total of 25 μg protein of each sample were suspended in 50mM triethylammoniumbicarbonate (TEAB) pH 8.5, 6M Urea, 2M Thiourea, 1% SDS and reduced with 10 mM tris(2-carboxyethyl) phosphine for 1 h at 34 °C, alkylated with 20 mM iodoacetamide for 45 min in the dark, then quenched with a final concentration of 32 mM Dithiothreitol (DTT). Each sample was digested separately using the S-Trap Micro Spin column (Protifi, Huntington NY) [52]. After quenching, 12% phosphoric acid was added to a final concentration of 1%, followed by 1:7 dilution (v/v) with 90% methanol, 0.1M TEAB pH 8.5. The samples were loaded into a S-Trap Micro spin column and centrifuged at 4000g for 30 sec, then washed three times with 150 μl of 90% methanol, 0.1 M TEAB pH 8.5. Digestion was performed with 25 μl trypsin at 100 ng/μl (1:10 w/w) in 50 mM TEAB pH 8.5 added to the top of the spin column. Spin columns were incubated overnight (16 hr) at 37 °C. Following incubation, the digested peptides were eluted off the S-trap column sequentially with 40 μl each of 50 mM TEAB pH 8.5, 0.2% formic acid, 50% acetonitrile-0.2% formic acid. Three eluates were pooled together and dried before reconstituting in 100 μl water and re-dried to remove residual formic acid.

Prior to labeling each sample was reconstituted into 30 μl 0.1M TEAB pH 8.5. The TMT 16-plex label was reconstituted with 15 μl of anhydrous acetonitrile prior to labeling, added to each of the 30 μl tryptic digest samples (1:6.6 w/w ratio peptide to

TMT label), and incubated for 1 hour at room temperature. The labeled peptides from the 15 samples were pooled together. The pooled peptides from each replicate were then evaporated to dryness and cleanup by solid phase extraction (SPE) on MCX Cartridges (Waters, Milford, MA). Labeling incorporation was checked using Orbitrap Eclipse Thermo-Fisher Scientific, San Jose, CA). The eluted tryptic peptides were evaporated to dryness, and fractionated using a Dionex UltiMate 3000 HPLC system with the built-in micro fraction collection option in its autosampler and UV detection (Thermo Scientific, Sunnyvale, CA) as described [48-51]. The TMT-labeled tryptic peptides were reconstituted in buffer A (20 mM ammonium formate pH 9.5 in water), and loaded onto an XTerra MS C18 column (3.5 μm, 2.1x 150 mm) from Waters, (Milford, MA) with 20 mM ammonium formate (NH_4FA), pH 9.5 as buffer A and 80% ACN/20% 20 mM NH_4FA as buffer B. The LC was performed using a gradient from 10-45% of buffer B in 30 minutes at a flow rate 200 μL/min. Forty-eight fractions were collected at 1-minute intervals and pooled into a total of 10 fractions based on the UV absorbance at 214 nm and with multiple fraction concatenation strategy [53]. Each of the 10 fractions was dried and reconstituted in 100 μL of 2% ACN/0.5% FA for nanoLC-MS/MS analysis.

The nanoLC-MS/MS analysis was carried out using an Orbitrap Eclipse (Thermo-Fisher Scientific, San Jose, CA) mass spectrometer equipped with a nanospray Flex Ion Source coupled with the UltiMate 3000 RSLCnano (Dionex, Sunnyvale, CA). Each reconstituted fraction (3.5 µL = 0.7 μg for global proteomics fractions) was injected onto a PepMap C-18 RP nano trap column (5 μm, 100 μm × 20 mm, Dionex) at 20 µL/min flow rate for rapid sample loading and separated on a PepMap C-18 RP

nano column (2 μm, 75 μm x 25 cm). The column was equilibrated with 2% acetonitrile (ACN) in 0.1% aqueous formic acid (eluant A) prior to each run. The labeled peptides were eluted in a 120 min gradient of 5% to 32% eluant B containing 95% ACN in 0.1% formic acid at 300 nL/min, followed by an 8-min ramping to 90% B, a 7-min hold, and 21-min re-equilibration with 2% ACN-0.1% FA prior to the next run. The Orbitrap Eclipse was operated in positive ion mode with nanospray voltage set at 1.9 kV and source temperature at 300 °C. External calibration for FT, IT and quadrupole mass analyzers was performed. Raw MS data files for all the fractions were acquired using a real-time search (RTS) synchronous precursor selection (SPS) MS^3 workflow as reported previously [48]. Specifically, the RTS MS^3 workflow consisted of 2.5 second "Top Speed" data-dependent CID-MS/MS scans (for peptide identifications by RTS) that enabled to trigger SPS of 10 MS^2 product ions for subsequent MS^3 in FT. In RTS mode, the *Mycobacterium tuberculosis* NCBI database downloaded November 2021 which contains 417575 sequences were imported as the FASTA database with trypsin as the enzyme for real-time spectral database search respectively for the samples from corresponding species. The search parameters included: TMTpro modifications on lysine and N-terminal amines (Δmass 304.2071), carbamidomethyl modification of cysteine (Δmass 57.0215), and maximum 2 variable methionine oxidation per peptide, and 1 missed cleavage. A maximum search time for 35 ms allowed for the RTS MS^3 searching. The MS^3 scan was carried out using a mass range of 110-500 m/z, an MS isolation window of 1.1 m/z and MS^2 isolation window of 2.0 m/z were used. A resolving power of 50,000 at MS^3 with a normalized collision energy of 55% was used for peptide quantitation. Other parameters included 200%

normalized AGT target and 120 ms for maximum injection time. Dynamic exclusion parameters were set at 1 within 50s exclusion duration with ±10 ppm exclusion mass window. All data were acquired under Xcalibur 4.3 operation software in Orbitrap Eclipse (Thermo Fisher Scientific).

Data processing, protein identification and data analysis

All raw MS spectra were processed and searched using the Sequest HT search engine within the Proteome Discoverer 2.5 (PD 2.5, Thermo). A *Mycobacterium tuberculosis* str. Erdman ATCC 35801 NCBI database comprised of 4,222 sequences was used for post-MS database searches. The default search settings used for 16-plex TMT quantitative processing and protein identification in PD 2.5 searching software were: two mis-cleavage for full trypsin with fixed carbamidomethyl modification of cysteine, fixed 16-plex TMT modifications on lysine and N-terminal amines along with variable modifications of methionine oxidation, deamidation on asparagine/glutamine residues and protein N-terminal acetylation. The peptide mass tolerance and fragment mass tolerance values were 10 ppm for MS survey scan, 0.6 Da for MS^2 and 20 ppm for MS^3, respectively. Identified peptides were further filtered for maximum 1% FDR using the Percolator algorithm in PD 2.5 along with additional peptide confidence set to high and peptide mass accuracy ≤5 ppm. The TMT16-plex quantification method within Proteome Discoverer 2.5 software was used to calculate the reporter ion abundances in MS^3 spectra that were corrected for the isotopic impurities. Both unique and razor peptides were used for quantitation. Signal-to-noise (S/N) values were used to represent the reporter ion abundance with a co-isolation threshold of 50% and an average reporter S/N (intensity) threshold of ≥10 used for

quantitation spectra. The intensities of peptides, which were summed from the intensities of the peptide-spectrum match (PSM), were summed to represent the abundance of the proteins. For relative ratio between the two groups, normalization on total peptide amount for each sample was applied. T-test was used for p-values calculation of the reported ratios. The search result including ratio, peptide abundance for each sample was output to Microsoft Excel software for further data analysis.

Western blot analysis

To obtain whole cell lysates for western blot analysis, Mtb strains were cultured in 40 ml of 7H9 OADC + 0.05% tyloxapol to an OD_{600} of 0.6. Bacteria were harvested through centrifugation and fixed for 1 hour with 4% PFA. Cells were washed with PBS 0.05% tyloxapol and lysed in 1% SDS using sonication. Where applicable, 20 μg/ml chloramphenicol was added 2 days prior to harvesting. After separation via SDS-PAGE, proteins were transferred to a nitrocellulose membrane. Antibodies for GroEL were obtained from BEI resources and anti-MceG antibodies were generated as previously described [8]. Antibodies for Mce1A, Mce1D, and Mce1E were a gift from Christopher Sassetti [54]. Antibodies for Mce4A and Mce4E were a gift from Miriam Braunstein [14].

Isolation of RNA and qPCR analysis

RNA was purified from WT, *mceG* mutant, complement, D188N or E189Q complement *M.tb* growing in exponential phase. Bacteria were pelleted and lysed in Trizol LS (Invitrogen) with 0.1 mm silica beads in a FastPrep-24 bead beating grinder (MP Biomedicals). The RNA was purified using Trizol LS per manufacturer

instructions with the addition of a second chloroform extraction and a second ethanol wash. The DNA was digested using TURBO DNA-free Kit (Invitrogen).

For relative quantification of gene expression, cDNA was generated from 250 ng of RNA using iScript cDNA synthesis kit (Biorad) and real-time PCR was performed using the iTaq SYBR Green kit (Biorad) on the 7500 Fast Real-Time PCR System (Applied Biosystems). Gene-specific primers were designed using Primer3 software. The sigma factor gene *sigA* (*Rv2703*) was used to normalize each sample and approximate fold induction compared to WT was calculated using the $2^{-\Delta CT}$ method [55]. Average and range of fold induction were calculated using the average and standard deviation of ΔCT from 4 experimental replicates, and statistical changes in ΔCT were determined using two-way ANOVA and Dunnett's multiple comparisons [56].

Mouse infection studies

Animal work was approved by Cornell University IACUC (protocol number 2013-0030). All protocols conform to the USDA Animal Welfare Act, institutional policies on the care and humane treatment of animals, and other applicable laws and regulations. Six to eight-week-old female BALB/cJ wild type mice Jackson Laboratories were infected with 1000 CFU of Mtb strains via an intranasal delivery method as described [57]. The mice were anesthetized with isoflurane and 25 µl of bacteria were introduced into both nares. At sacrifice, the lungs were removed, and half of the lungs were fixed in 4% PFA overnight for histology studies, while another half was used for bacterial load quantification. For the latter, lungs were homogenized

in PBS 0.05% Tween-80 and plated on 7H10 OADC agar. CFU were quantified after 3–4 weeks incubation at 37°C.

Data availability: All data are contained within the article. Material described is available upon request from the corresponding author.

Acknowledgements: We thank the Proteomic and Metabolomics Facility of Cornell University for generating the mass spectrometry data and the funding support from HHMI Transformative Technology 2019 program for the Orbitrap Eclipse system. We thank the Miriam Braunstein lab for the Mce4 antibodies.
This research was supported by National Institutes of Health Grants RO1130018 (B.C.V.)

Author contributions: R. A. F., K. M. W., and E. V. N. conceptualization; R. A. F., K. M. W., and E. V. N. methodology; R. A. F., K. M. W., C. R. M., E. K. R., and C. M. K. writing - original draft; R. A. F., K. M. W., C.R.M., E.K.R., C.M.K., and T.L.S. investigation; H.S. and B.C.V. supervision; C. R. M., E. K. R., and C. M. K. writing - reviewing and editing.

Funding and additional information: This research was supported by National Institutes of Health Grants R01130018 (B. C. V.). The content is solely the responsibility of the authors and does not necessarily represent the official views of the National Institutes of Health.

Conflict of interest: All authors declare no conflicts of interest with the contents of this article.

SUPPLEMENTAL FIGURES

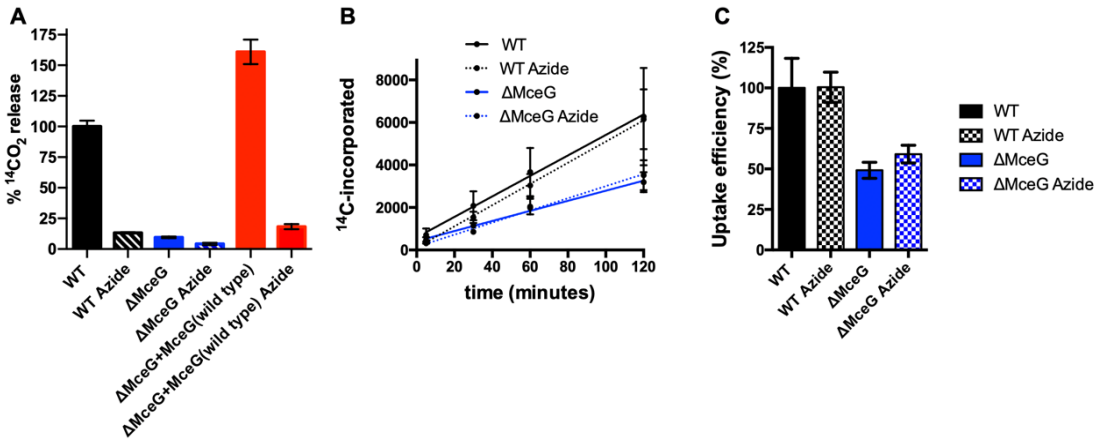

Figure S2.1. Azide inhibition of ^{14}C-cholesterol metabolism in Mtb. **(A)** Catabolic release of CO_2 from cholesterol in Mtb strains treated with sodium azide. **(B)** Rates of cholesterol import by Mtb cells treated with sodium azide. (**C**) Whole cell quantification of the rate of cholesterol import by Mtb cells. Data are SEM from ≥ 2 technical replicates each from ≥ 2 biological replicates.

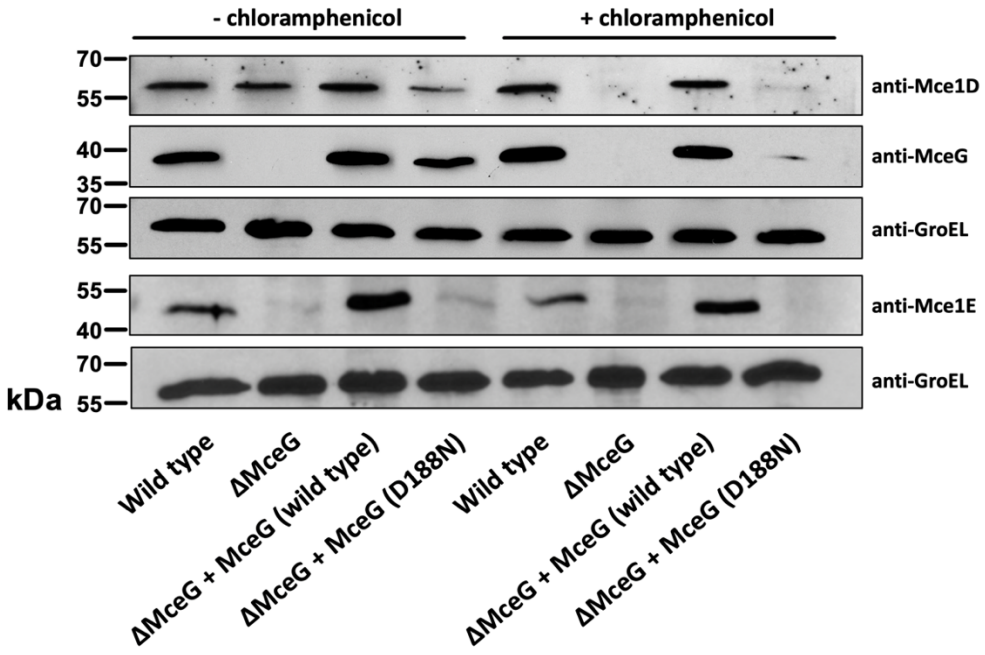

Figure S2.2. Mce1 proteins are actively degraded in the absence of MceG. Mtb whole cell lysates from cells treated with +/- 20 μg/ml chloramphenicol 2 days prior to harvesting were probed with antibodies specific to protein of the Mce transporters and GroEL2 as the loading control. Western blots depicted are representative images of two independent replicates.

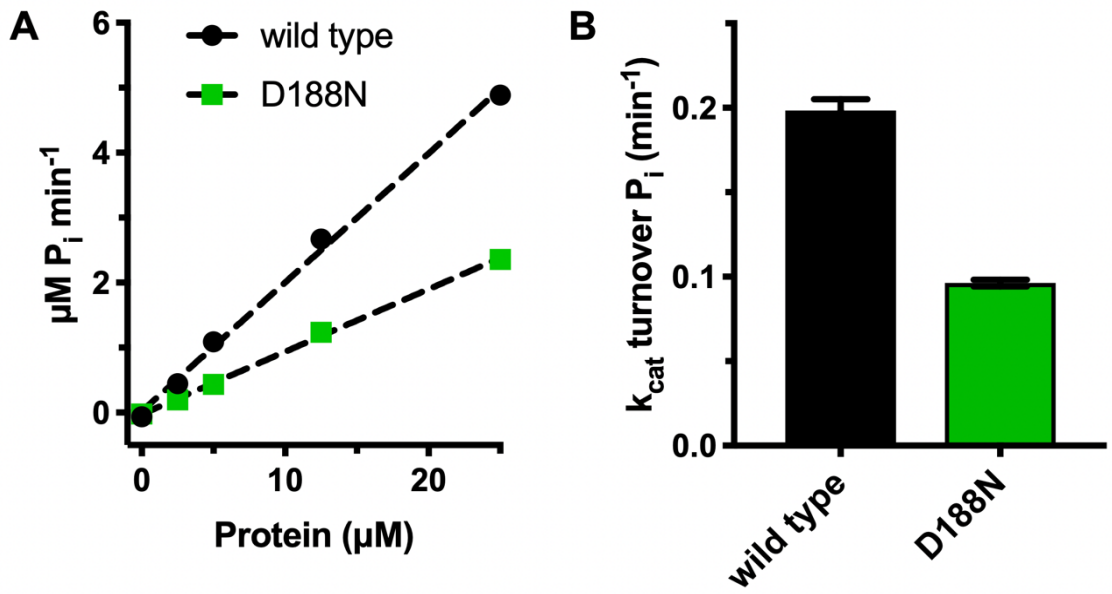

Figure S2.3. MceG ATPase activity (A) ATPase activity of recombinant wild type MceG and catalytically inactive MceG (D188N). The kinetics of phosphate release from ATP were measured over five protein concentrations, with the average of six technical replicates for each concentration and plotted in μM P_i released min^{-1}. (**B**) k_{cat} values calculated from the rates displayed in panel B. Error bars show SEM of average turnover rate for WT and D188N mutant.

REFERENCES

1. *World Health Organization. Global Tuberculosis Report 2021.* WHO.

2. Russell, D.G., C.E. Barry, 3rd, and J.L. Flynn, *Tuberculosis: what we don't know can, and does, hurt us.* Science, 2010. **328**(5980): p. 852-6.

3. Ehrt, S., D. Schnappinger, and K.Y. Rhee, *Metabolic principles of persistence and pathogenicity in Mycobacterium tuberculosis.* Nat Rev Microbiol, 2018. **16**(8): p. 496-507.

4. Wilburn, K.M., R.A. Fieweger, and B.C. VanderVen, *Cholesterol and fatty acids grease the wheels of Mycobacterium tuberculosis pathogenesis.* Pathog Dis, 2018. **76**(2).

5. Jackson, M., et al., *Transporters Involved in the Biogenesis and Functionalization of the Mycobacterial Cell Envelope.* Chem Rev, 2021. **121**(9): p. 5124-5157.

6. Ates, L.S., et al., *Essential Role of the ESX-5 Secretion System in Outer Membrane Permeability of Pathogenic Mycobacteria.* PLoS Genet, 2015. **11**(5): p. e1005190.

7. Wang, Q., et al., *PE/PPE proteins mediate nutrient transport across the outer membrane of Mycobacterium tuberculosis.* Science, 2020. **367**(6482): p. 1147-1151.

8. Nazarova, E.V., et al., *Rv3723/LucA coordinates fatty acid and cholesterol uptake in Mycobacterium tuberculosis.* 2017. **6**.

9. Pandey, A.K. and C.M. Sassetti, *Mycobacterial persistence requires the utilization of host cholesterol.* Proceedings of the National Academy of Sciences, 2008. **105**(11): p. 4376-4380.

10. Casali, N. and L.W. Riley, *A phylogenomic analysis of the Actinomycetales mce operons.* BMC Genomics, 2007. **8**: p. 60.

11. Joshi, S.M., et al., *Characterization of mycobacterial virulence genes through genetic interaction mapping.* Proceedings of the National Academy of Sciences, 2006. **103**(31): p. 11760-11765.

12. Nazarova, E.V., et al., *The genetic requirements of fatty acid import by Mycobacterium tuberculosis within macrophages.* Elife, 2019. **8**.

13. Perkowski, E.F., et al., *An orphaned Mce-associated membrane protein of Mycobacterium tuberculosis is a virulence factor that stabilizes Mce transporters.* Mol Microbiol, 2016. **100**(1): p. 90-107.

14. Rank, L., L.E. Herring, and M. Braunstein, *Evidence for the Mycobacterial Mce4 Transporter Being a Multiprotein Complex.* J Bacteriol, 2021. **203**(10).

15. Wilkens, S., *Structure and mechanism of ABC transporters.* F1000Prime Rep, 2015. **7**: p. 14.

16. Mohn, W.W., et al., *The actinobacterial mce4 locus encodes a steroid transporter.* J Biol Chem, 2008. **283**(51): p. 35368-74.

17. Dubos, R.J. and B.D. Davis, *Factors affecting the growth of tubercule bacilli in liquid media.* J Exp Med, 1946. **83**(5): p. 409-23.

18. [preprint] Chen, J., Fruhauf, A., Fan, C., Ponce, J., Ueberheide, B., Bhabha, G., *et al*., *Structure of an endogenous mycobacterial MCE lipid transporter.* bioRxiv, 2022. **10.1101/2022.12.08.519548**

19. Kolich, L.R., et al., *Structure of MlaFB uncovers novel mechanisms of ABC transporter regulation.* Elife, 2020. **9**.

20. Thong, S., et al., *Defining key roles for auxiliary proteins in an ABC transporter that maintains bacterial outer membrane lipid asymmetry.* 2016. **5**.

21. ter Beek, J., A. Guskov, and D.J. Slotboom, *Structural diversity of ABC transporters.* J Gen Physiol, 2014. **143**(4): p. 419-35.

22. Forrellad, M.A., et al., *Study of the in vivo role of Mce2R, the transcriptional regulator of mce2 operon in Mycobacterium tuberculosis.* BMC Microbiol, 2013. **13**: p. 200.

23. Santangelo, M.P., et al., *Mce3R, a TetR-type transcriptional repressor, controls the expression of a regulon involved in lipid metabolism in Mycobacterium tuberculosis.* Microbiology (Reading), 2009. **155**(Pt 7): p. 2245-2255.

24. Urbatsch, I.L., et al., *Mutational analysis of conserved carboxylate residues in the nucleotide binding sites of P-glycoprotein.* Biochemistry, 2000. **39**(46): p. 14138-49.

25. Schaupp, A., et al., *Processing of proteins by the molecular chaperone Hsp104.* J Mol Biol, 2007. **370**(4): p. 674-86.

26. Ekiert, D.C., et al., *Architectures of Lipid Transport Systems for the Bacterial Outer Membrane.* Cell, 2017. **169**(2): p. 273-285.e17.

27. Jiang, J.H., et al., *Identification of Novel Acinetobacter baumannii Host Fatty Acid Stress Adaptation Strategies.* mBio, 2019. **10**(1).

28. Parsons, J.B., et al., *Membrane disruption by antimicrobial fatty acids releases low-molecular-weight proteins from Staphylococcus aureus.* J Bacteriol, 2012. **194**(19): p. 5294-304.

29. Beavers, W.N., et al., *Arachidonic Acid Kills Staphylococcus aureus through a Lipid Peroxidation Mechanism.* mBio, 2019. **10**(5).

30. Abrahams, G.L., et al., *Pathway-selective sensitization of Mycobacterium tuberculosis for target-based whole-cell screening.* Chem Biol, 2012. **19**(7): p. 844-54.

31. Vandal, O.H., et al., *Cytosolic phospholipase A2 enzymes are not required by mouse bone marrow-derived macrophages for the control of Mycobacterium tuberculosis in vitro.* Infect Immun, 2006. **74**(3): p. 1751-6.

32. García, J., et al., *Mycobacterium tuberculosis Rv2536 protein implicated in specific binding to human cell lines.* Protein Sci, 2005. **14**(9): p. 2236-45.

33. Chitale, S., et al., *Recombinant Mycobacterium tuberculosis protein associated with mammalian cell entry.* Cell Microbiol, 2001. **3**(4): p. 247-54.

34. Anantharaman, V. and L. Aravind, *Evolutionary history, structural features and biochemical diversity of the NlpC/P60 superfamily of enzymes.* Genome Biol, 2003. **4**(2): p. R11.

35. Mavrici, D., et al., *Mycobacterium tuberculosis FtsX extracellular domain activates the peptidoglycan hydrolase, RipC.* Proc Natl Acad Sci U S A, 2014. **111**(22): p. 8037-42.

36. Parthasarathy, G., et al., *Rv2190c, an NlpC/P60 family protein, is required for full virulence of Mycobacterium tuberculosis.* PLoS One, 2012. **7**(8): p. e43429.

37. Varrot, A., et al., *Mycobacterium tuberculosis strains possess functional cellulases.* J Biol Chem, 2005. **280**(21): p. 20181-4.

38. Trivedi, A., et al., *Thiol reductive stress induces cellulose-anchored biofilm formation in Mycobacterium tuberculosis.* Nat Commun, 2016. **7**: p. 11392.

39. de Carvalho, L.P., et al., *Metabolomics of Mycobacterium tuberculosis reveals compartmentalized co-catabolism of carbon substrates.* Chem Biol, 2010. **17**(10): p. 1122-31.

40. Barry, C.E., 3rd, et al., *The spectrum of latent tuberculosis: rethinking the biology and intervention strategies.* Nat Rev Microbiol, 2009. **7**(12): p. 845-55.

41. Russell, D.G., et al., *Mycobacterium tuberculosis Wears What It Eats.* Cell Host & Microbe, 2010. **8**(1): p. 68-76.

42. Beites, T., et al., *Multiple acyl-CoA dehydrogenase deficiency kills Mycobacterium tuberculosis in vitro and during infection.* Nat Commun, 2021. **12**(1): p. 6593.

43. VanderVen, B.C., et al., *Novel inhibitors of cholesterol degradation in Mycobacterium tuberculosis reveal how the bacterium's metabolism is constrained by the intracellular environment.* PLoS Pathog, 2015. **11**(2): p. e1004679.

44. Mann, F.M., B.C. VanderVen, and R.J. Peters, *Magnesium depletion triggers production of an immune modulating diterpenoid in Mycobacterium tuberculosis.* Mol Microbiol, 2011. **79**(6): p. 1594-601.

45. Lee, W., et al., *Intracellular Mycobacterium tuberculosis exploits host-derived fatty acids to limit metabolic stress.* J Biol Chem, 2013. **288**(10): p. 6788-800.

46. Nazarova, E.V., et al., *Flow Cytometric Quantification of Fatty Acid Uptake by Mycobacterium tuberculosis in Macrophages.* Bio-protocol, 2018. **8**(4): p. e2734.

47. Podinovskaia, M., et al., *Infection of macrophages with Mycobacterium tuberculosis induces global modifications to phagosomal function.* Cell Microbiol, 2013. **15**(6): p. 843-59.

48. Fu, Q., et al., *Comparison of MS(2), synchronous precursor selection MS(3), and real-time search MS(3) methodologies for lung proteomes of hydrogen sulfide treated swine.* Anal Bioanal Chem, 2021. **413**(2): p. 419-429.

49. Liu, Z., et al., *Proteomics analysis of lung reveals inflammation and cell death induced by atmospheric H(2)S exposure in pig.* Environ Res, 2020. **191**: p. 110204.

50. Qin, L., et al., *Adaption of Roots to Nitrogen Deficiency Revealed by 3D Quantification and Proteomic Analysis.* Plant Physiol, 2019. **179**(1): p. 329-347.

51. Yang, Y., et al., *Altered succinylation of mitochondrial proteins, APP and tau in Alzheimer's disease.* Nat Commun, 2022. **13**(1): p. 159.

52. Yang, Y., E. Anderson, and S. Zhang, *Evaluation of six sample preparation procedures for qualitative and quantitative proteomics analysis of milk fat globule membrane.* Electrophoresis, 2018. **39**(18): p. 2332-2339.

53. Yang, Y., et al., *Evaluation of different multidimensional LC-MS/MS pipelines for isobaric tags for relative and absolute quantitation (iTRAQ)-based proteomic analysis of potato tubers in response to cold storage.* J Proteome Res, 2011. **10**(10): p. 4647-60.

54. Feltcher, M.E., et al., *Label-free Quantitative Proteomics Reveals a Role for the Mycobacterium tuberculosis SecA2 Pathway in Exporting Solute Binding Proteins and Mce Transporters to the Cell Wall.* Mol Cell Proteomics, 2015. **14**(6): p. 1501-16.

55. Livak, K.J. and T.D. Schmittgen, *Analysis of relative gene expression data using real-time quantitative PCR and the 2(-Delta Delta C(T)) Method.* (1046-2023 (Print)).

56. Yuan, J.S., et al., *Statistical analysis of real-time PCR data.* (1471-2105 (Electronic)).

57. Sukumar, N., et al., *Exploitation of Mycobacterium tuberculosis reporter strains to probe the impact of vaccination at sites of infection.* PLoS Pathog, 2014. **10**(9): p. e1004394.

CHAPTER 3

The *Mycobacterium tuberculosis* cell wall lipid PDIM facilitates the activation of PGE_2 production in macrophages*

*Fieweger RA, Montague CR, Pisu D, Islam MN, Roszkowski EK, Belisle JT, VanderVen BC. The *Mycobacterium tuberculosis* cell wall lipid PDIM facilitates the activation of PGE_2 production in macrophages. Manuscript in preparation.

ABSTRACT

Prostaglandin E_2 (PGE_2) can promote or suppress inflammation and during *Mycobacterium tuberculosis* (Mtb) infection, PGE_2 regulates both cell death pathways and the macrophage type I interferon (IFN) responses, yet how Mtb induces PGE_2 production remains poorly understood. Here, we demonstrate that the cell wall lipid, phthiocerol dimycocerosate (PDIM), is required to stimulate PGE_2 synthesis during Mtb infection. Mtb mutants lacking PDIM fail to stimulate the production of the inflammatory eicosanoid PGE_2 in the lungs of mice and in macrophages *ex vivo*. The process of stimulating PGE_2 production in macrophages can be reconstituted by providing macrophages particles coated with Mtb total lipids. PDIM-mediated stimulation of PGE_2 production occurs independent of signaling through IL-1β and the NLRP3 inflammasome complex. Additionally, PDIM-mediated stimulation of PGE_2 production requires phagosomal membrane rupture and is dependent on the ESX-1 secretory protein, ESAT-6 for this activity. Importantly, PDIM producing Mtb do not induce a robust IFN response suggesting that cell intrinsic PGE_2 counter-regulates the macrophage IFN response following phagosomal rupture. This work reveals a new aspect of Mtb sensing in the cytosol of macrophages and provides a more complete understanding of critical events in Mtb cell wall homeostasis.

INTRODUCTION

Mycobacterium tuberculosis (Mtb), the etiologic agent of tuberculosis remains a significant global health problem that causes ~10 million new cases of infections and ~1.6 million deaths every year [1]. This devastating pathogen has evolved over millennia within the human population and has built an arsenal of protein and lipid virulence factors that manipulate the host immune response facilitating long-term infection.

While Mtb is thought to mainly live within endosomal compartments, a subset of intracellular Mtb are capable of rupturing phagosome membranes resulting in deposition of Mtb into the macrophage cytosol [2-4]. It is thought that the principle bacterial factor responsible for phagosome rupture is the secreted effector protein of the Type VII secretion system, ESAT-6 [3, 5, 6]. Once in the cytosol, Mtb triggers the DNA-dependent cytosolic surveillance pathway (CSP) leading to production of type I interferons (IFN) and macrophage necrotic cell death [5, 7]. The presence of type I IFNs have also been shown to aid Mtb in establishment of infection as these cytokines dampen production of IL-1β as well as an important product of IL-1β signaling, prostaglandin E_2 (PGE_2) [8]. Thus, a complex counter-regulatory loop exists where the levels of IFNs, IL-1β, and PGE_2 all impact macrophage cell death and the outcome of Mtb infection [9].

More recently, an important lipid of the Mtb cell envelope, phthiocerol dimycocerosate (PDIM), has also been implicated in phagosomal rupture and escape. PDIM is essential for Mtb pathogenesis and is thought to perturb the host at multiple stages of infection [10]. Reports indicate that Mtb mutants lacking PDIM are unable to

gain access to the cytosol or induce production of IFNs [4, 11-13]. ESAT-6 has been shown to have pore-forming capabilities and it is thought that PDIM is required for ESAT-6 activity [14, 15]. Additionally, ESAT-6- and PDIM-mediated phagosomal rupture and bacterial escape into the cytosol is correlated with necrotic cell death of the infected host cell [3, 12]. Necrotic cell death is associated with bacterial dissemination; therefore, it is hypothesized that Mtb utilizes ESAT-6 in conjunction with PDIM to spread to new host cells.

Despite the importance of PGE_2 signaling, phagosomal rupture, and cytosolic sensing of Mtb, our understanding of how these processes impact macrophage responses during Mtb infection remains incomplete. To address these gaps, we reevaluated the role PDIM plays in Mtb pathogenesis.

RESULTS

PDIM is required to stimulate PGE_2 production in vivo.

Elevated levels of type 1 IFNs correlate with active TB disease in humans [16] and in the mouse model of TB disease, PGE_2 negatively regulates the production of type 1 IFNs [8]. Recent reports indicate that cytosolic *Listeria monocytogenes* is efficiently detected by macrophages and is associated with elevated levels of PGE_2 [17]. Given the recently proposed role for PDIM in regulating the production of type I IFNs, we sought to evaluate the effect PDIM may have on PGE_2 production. To begin, we screened colonies of wild type Erdman for isolates lacking PDIM. We obtained an isolate that contains a single base pair deletion ~3.6 kilobases into *mas*/*rv2940c* resulting in an early stop codon immediately downstream of the deletion. The product of *mas*/*rv2940c* is responsible for synthesizing the mycocerosic acid that is esterified onto the phthiocerol backbone of PDIM. This isolate was chosen because we expected that this genetic lesion would induce limited to no polar effects on surrounding genes at this locus. We designated this isolate $mas^{Pro1223delC}$. Radio-TLC analysis of total lipid extracts from $mas^{Pro1223delC}$ following radiolabeling with ^{14}C-propionate confirmed that the $mas^{Pro1223delC}$ mutant does not synthesize PDIM (Figure 3.1A). PDIM production was restored when the mutant strain was complemented with expression of a full-length *mas*/*rv2940c* gene and this strain was designated mas comp (Figure 3.1A).

We next evaluated if PGE_2 is produced in a PDIM-dependent manner. BALB/c bone-marrow derived macrophages (BMMΦ) were infected with wild type, $mas^{Pro1223delC}$, and mas comp bacteria and levels of PGE_2 secreted by macrophages

was quantified by enzyme-linked immunosorbent assay or mass spectrometry after 24 and 48 hours. At both timepoints, PGE_2 was induced by wild type and mas comp bacteria but not the *mas*^{Pro1223delC} mutant (Figure 3.1B and 3.1C). Bacterial burden was assessed and similar numbers of colony forming units (CFUs) were recovered from BMMΦ infected with each strain at 0- and 24-hours post-infection; a slight, but significant decrease in CFUs was seen in *mas*^{Pro1223delC} infected BMMΦ at 48 hours post-infection (Figure 3.1D). We conclude that PGE_2 induction in macrophages during Mtb infection is dependent on bacterial production of PDIM and the lack of PGE_2 production in the absence of PDIM is not due to lack of bacterial replication.

Next, we obtained total lipid extracts from wild type, *mas*^{Pro1223delC}, and mas comp bacteria and coupled the lipids onto 3.0-micron C18 reverse phase beads for delivery into macrophage phagosomes [18]. BALB/c BMMΦ were treated with lipid-coated beads and levels of PGE_2 induction were quantified after 24 hours. Beads containing lipids from wild type and mas comp bacteria induced PGE_2 production in BMMΦ, while lipids from the *mas*^{Pro1223delC} mutant did not (Figure 3.1E). These findings provide further support that PDIM is required for PGE_2 production in infected macrophages.

Lastly, PDIM deficient strains are known to be attenuated *in vivo* [19-21], so we assessed the requirement for PDIM in PGE_2 production early in infection using the mouse model. BALB/c mice were infected with wild type, *mas*^{Pro1223delC}, and mas comp bacteria and 3 days post-infection levels PGE_2 production and bacterial burden in mouse lungs were quantified. PGE_2 was induced in a PDIM dependent manner and similar numbers of bacteria were recovered from *mas*^{Pro1223delC} and mas comp infected

mice, but there was a small, but significant increase in bacterial burden in wild type infected mice (Figure 3.1F and 3.1G). Overall, we conclude that PDIM is necessary for production of PGE_2 in macrophages and *in vivo* during early stages of Mtb infection.

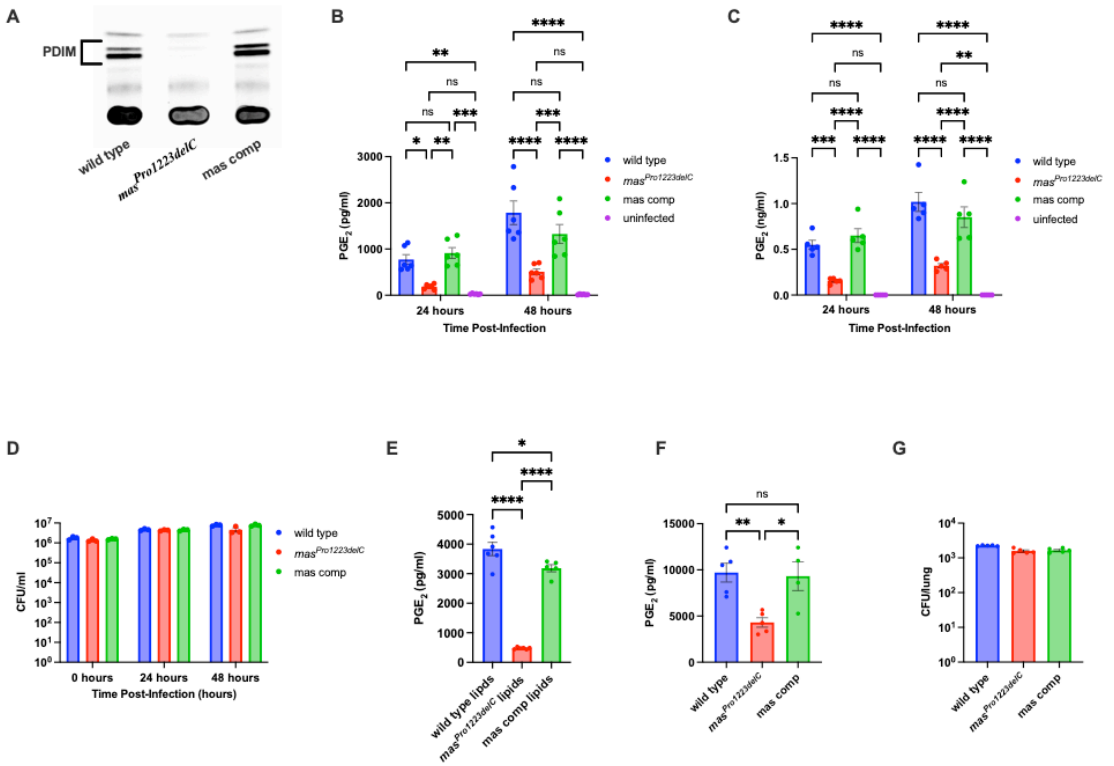

Figure 3.1. PDIM is required to stimulate PGE_2 production in macrophages and *in vivo*. **(A)** TLC autoradiogram of total lipid extracts isolated from Mtb following labeling with ^{14}C-propionate. Equal counts of Mtb lipids (20K CPM) were resolved in a petroleum ether:ethyl acetate (98:2 v/v). Bands corresponding to PDIM are labeled. **(B)** PGE_2 levels secreted by BALB/c BMMΦ infected with wild type, *mas*^{Pro1223delC}, and mas comp Mtb for 24-hours were quantified by ELISA and **(C)** mass-spectrometry. **(D)** Colony forming units of wild type, *mas*^{Pro1223delC}, and mas comp bacteria from infected BALB/c BMMΦ individually plotted immediately after infection and 24-hours and 48-hours post-infection. **(E)** PGE_2 levels secreted by BALB/c BMMΦ treated with C18 beads conjugated with lipid extracts from wild type, *mas*^{Pro1223delC}, and mas comp Mtb for 24-hours were quantified by ELISA. **(F)** PGE_2 levels in the lung homogenates of BALB/c mice infected with wild type, *mas*^{Pro1223delC}, and mas comp Mtb were quantified by ELISA 3 days post-infection.

(**G)** Colony forming units of wild type *mas*^{Pro1223delC}, and mas comp bacteria from the lungs of mice 3 days post-infection individually plotted. Data (n ≥ 5) ± SEM. Significance was calculated using a two-way ANOVA with Dunnett's multiple comparisons test (B-D) or one-way ANOVA with Dunnett's multiple comparisons test (E-G) (**** $P < 0.0001$) ns = not significant.

PDIM-mediated activation of PGE$_2$ synthesis in macrophages occurs independent of IL-1β signaling and IL-1β.

Upon infection with Mtb, toll-like receptors (TLRs) are activated, and in conjunction with the TLR adapter protein MYD88, can lead to activation the transcription factor NF-κB which induces production of pro-IL-1β [22, 23]. Pro-IL-1β is proteolytically cleaved into an active and secreted form by the NLRP3 inflammasome [23]. Importantly, signaling to neighboring macrophages through the IL-1 receptor (IL-1R) leads to the lipase-dependent release of arachidonic acid from membrane phospholipids and expression of cyclooxygenase-2 (COX-2), thereby resulting in conversion of arachidonic acid into PGE_2 via COX-2 [24, 25]. Thus, we sought to determine if the PDIM-dependent induction of PGE_2 is dependent on TLR activation or IL-1β signaling.

Macrophages lacking the IL-1α/β receptor (IL-1R$^{-/-}$), or the major Toll-like receptor adaptor (MYD88$^{-/-}$) were infected with wild type, *mas*^{Pro1223delC}, and mas comp bacteria. IL-1β, PGE_2, and levels of bacterial burden were quantified after 24 hours of infection. We found that IL-1β was induced following infection in wild type and IL-1R$^{-/-}$ macrophages infected with wild type and mas comp bacteria and IL-1β was not induced in cells infected with *mas*^{Pro1223delC} bacteria (Figure 3.2A). While infection with wild type and mas comp Mtb induces IL-1β production (Figure 3.2A)

the PDIM-dependent production of PGE_2 by the macrophages is not impacted by IL-1β signaling in cells that cannot respond to this cytokine (Figure 3.2B). Additionally, we confirmed that macrophages from different wild type mouse backgrounds (BALB/c and C57BL/6) produce PGE_2 in a PDIM-dependent manner (Figure 3.2B).

In contrast, PGE_2 was not induced by $MYD88^{-/-}$ BMMΦ infected with any strain indicating that Toll-like receptor stimulation is required to initiate the response resulting in PGE_2 production (Figure 3.2B). In these studies, similar levels of bacteria were recovered from wild type, $mas^{Pro1223delC}$, and mas comp infected wild type, $IL\text{-}1R^{-/-}$, and $MYD88^{-/-}$ C57BL/6 BMMΦ immediately after infection however there was a small, but significant increase in bacteria recovered from mas comp infected BMMΦ compared to wild type and $mas^{Pro1223delC}$ infected cells at 24-hours post infection (Figure 3.2C and 3.2D). Taken together, these findings imply PDIM-dependent induction of PGE_2 requires the adapter protein MYD88 and therefore TLR activation, but it does not require IL-1β or IL-1β signaling. Even though IL-1β is induced in a PDIM-dependent manner, when BMMΦ are no longer able to sense IL-1β due to the absence of IL-1R, they still produce PGE_2 in a PDIM dependent manner to levels similar to wild type BMMΦ suggesting PGE_2 production occurs regardless of the presence of IL-1β or IL-1β signaling.

Lastly, since pro-IL-1β is cleaved to IL-1β by the NLRP3 inflammasome, we assessed if PDIM-mediated PGE_2 production required activation of the NLRP3 inflammasome. Wild type BALB/c BMMΦ were treated with wild type Mtb lipid-coated beads in conjunction with the NLRP3 inflammasome inhibitor MCC950. Since cathepsin B is also required for IL-1β processing, BMMΦ were also treated with the

cathepsin B inhibitor CA-074 upon treatment with Mtb lipid-coated beads [26]. Wild type lipid-coated beads induced PGE_2 production to equal levels in the presence of MCC950 or dimethylsulfoxide (DMSO) vehicle control (Figure 3.2E). Surprisingly, induction of PGE_2 was reduced in the presence of wild type lipid-coated beads and CA-074 (Figure 3.2E). This suggests that the NLRP3 inflammasome is not required for PDIM-dependent activation of PGE_2 production, but cathepsin B is required and may play a role in PGE_2 production outside of IL-1β signaling.

In conclusion, PDIM-mediated activation of PGE_2 production requires TLR activation and cathepsin B activity but does not require the presence of IL-1β or IL-1β signaling. We hypothesize that PDIM-containing Mtb activate TLRs which trigger an unknown signaling cascade leading to PGE_2 production in macrophages.

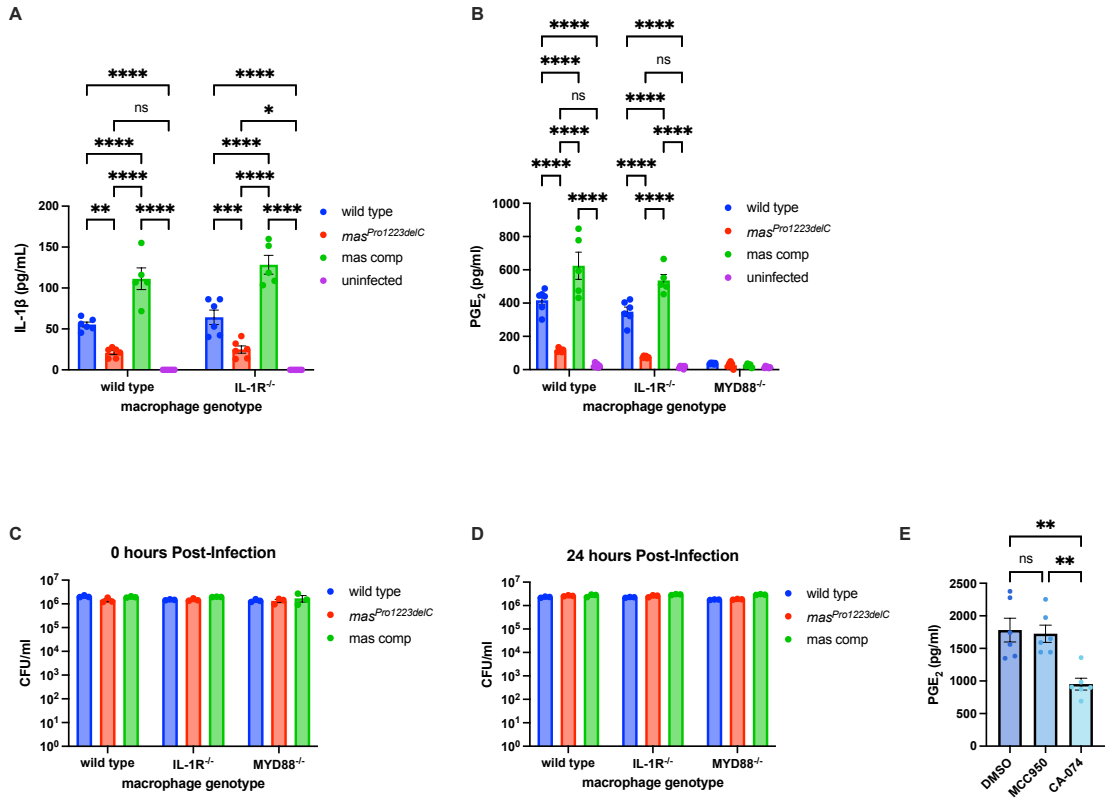

Figure 3.2. IL-1β signaling in not required for PDIM-dependent induction of PGE_2 in macrophages. (A) PGE_2 levels secreted by wild type, IL-1R$^{-/-}$, and MYD88$^{-/-}$ C57BL/6 BMMΦ infected with wild type, *mas*^{Pro1223delC}, and mas comp Mtb for 24 hours were quantified by ELISA. **(B)** IL-1β levels secreted by wild type and IL-1R$^{-/-}$ C57BL/6 BMMΦ infected with wild type, *mas*^{Pro1223delC}, and mas comp Mtb for 24 hours were quantified by ELISA. **(C)** Colony forming units of wild type *mas*^{Pro1223delC}, and mas comp bacteria from infected wild type, IL-1R$^{-/-}$, and MYD88$^{-/-}$ C57BL/6 BMMΦ individually plotted immediately after infection and **(D)** 24-hours post-infection. **(E)** PGE_2 levels secreted by BALB/c BMMΦ treated with C18 beads conjugated with lipid extracts from wild type Mtb for 24-hours were quantified by ELISA. BMMΦ were treated with either DMSO, 20 μM MCC950, or 20 μM CA-074 at time of bead addition. Data ($n \geq 5$) ± SEM. Significance was calculated using a two-way ANOVA with Dunnett's multiple comparisons test (A-D) or one-way ANOVA with Dunnett's multiple comparisons test (E) (**** $P < 0.0001$) ns = not significant.

ESAT-6 is required for PGE_2 production in macrophages.

The Type VII secreted effector protein ESAT-6 and PDIM are thought to work together to mediate phagosomal rupture and escape resulting in the induction of type I

IFNs. It follows then that ESAT-6 may be required for macrophage PGE_2 production. We generated ESAT-6 knockout strains of Mtb, designated Δ*ESAT-6,* that either retain the ability to produce PDIM (PDIM+) or have lost the ability for PDIM production (PDIM-). We complemented both the PDIM+ and PDIM- Δ*ESAT-6* mutants by expressing wild type ESAT-6 along with its chaperone protein CFP10. Radio-TLC analysis of total lipid extracts from these strains confirmed their PDIM status (Figure 3.3A). Additionally, mutants that lack ESAT-6 retain their ability to export PDIM to the outer membrane (Figure 3.3B). For this experiment, an Δ*mmpL7* transporter mutant is used as a control since this mutant does not translocate PDIM to the bacterial cell surface even though the mutants still synthesizes PDIM [21].

Next, BALB/c BMMΦ were infected with wild type, Δ*ESAT-6* (PDIM+), Δ*ESAT-6* (PDIM-), Δ*ESAT-6* comp (PDIM+), and Δ*ESAT-6* comp (PDIM-) bacteria and PGE_2 production and bacterial burden was quantified after 24 hours. It was observed that wild type and Δ*ESAT-6* comp (PDIM+) induced similar levels of PGE_2 while Δ*ESAT-6* (PDIM+), Δ*ESAT-6* (PDIM-), and Δ*ESAT-6* comp (PDIM-) failed to induce production of PGE_2 (Figure 3.3C). Presence or absence of ESAT-6 or PDIM did not affect how efficiency bacteria were phagocytosed as assessed by CFUs recovered immediately after infection and did not affect bacterial survival at 24-hours post-infection, except for BMMΦ infected with Δ*ESAT-6* comp (PDIM+) where slightly, but significantly more bacteria were recovered (Figure 3.3D). Therefore, both the presence of PDIM and ESAT-6 is necessary for Mtb to induce production of PGE_2 during macrophage infection.

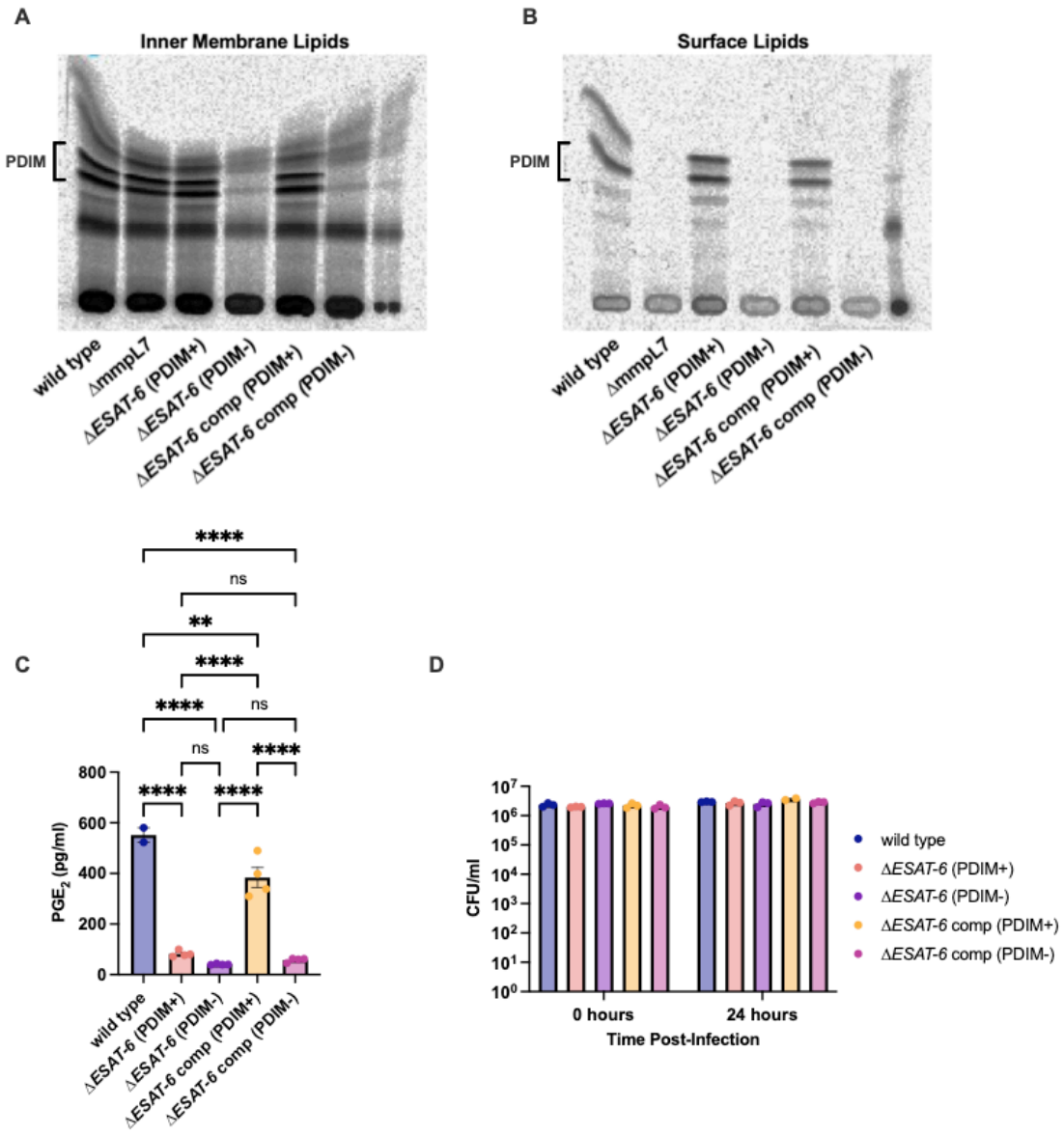

Figure 3.3. PDIM-mediated induction of PGE_2 in macrophages is dependent on ESAT-6. (A-B) TLC autoradiogram of (A) inner membrane lipids and (B) surface lipids extracted from Mtb following labeling with ^{14}C-propionate. Equal counts of Mtb lipids (20K CPM) were resolved in a petroleum ether:ethyl acetate (98:2 v/v). Bands corresponding to PDIM are labeled. **(C)** PGE_2 levels secreted by BALB/c BMMΦ infected with wild type, Δ*ESAT-6* (PDIM+), Δ*ESAT-6* (PDIM-), Δ*ESAT-6* comp (PDIM+), and Δ*ESAT-6* comp (PDIM-) Mtb for 24-hours were quantified by ELISA. **(D)** Colony forming units of wild type, Δ*ESAT-6* (PDIM+), Δ*ESAT-6* (PDIM-), Δ*ESAT-6* comp (PDIM+), and Δ*ESAT-6* comp (PDIM-) bacteria from infected BALB/c BMMΦ individually plotted immediately after infection and 24-hours post-infection. Data (n ≥ 5) ± SEM. Significance was calculated using a one-way ANOVA with Dunnett's multiple comparisons test (B) or two-way ANOVA with Dunnett's multiple comparisons test (C) (**** $P < 0.0001$) ns = not significant.

DISCUSSION

The current model states during infection Mtb can gain access to the macrophage cytosol and trigger production of type I IFNs via signaling through the DNA-dependent cytosolic surveillance pathway [5, 7, 11]. In turn, type I IFNs negatively regulate IL-1β and PGE_2 production, potentially facilitating environmental conditions that favor bacterial dissemination [8, 27]. Studies by Manzanillo *et al.* and Barczak *et al.* report that Mtb mutants lacking ESAT-6 and PDIM, respectively, are unable to induce type I IFN production whereas wild type Mtb can [5, 7, 11]. Neither study reported detecting PGE_2 production in infected macrophages, suggesting that induction of type I IFNs by Mtb leads to dampening of IL-1β and PGE_2 further supporting the model that type I IFNs and PGE_2 negatively regulate induction of one another during Mtb infection.

Surprisingly, in our studies PGE_2 production in macrophages and mice was detected upon infection with Mtb and required PDIM. In our hands, production of type I IFNs at the transcriptional or protein level in macrophages infected with Mtb was not detected (data not shown). While type I IFN production was not expected following infection with PDIM-deficient Mtb based on findings by Barczak *et al.*, it is possible that it was also not detected upon infection with PDIM-positive strains in the tested conditions due to the induction of PGE_2 as it has been proposed that PGE_2 negatively regulates induction of type I IFNs [8]. Further studies will need to show this definitively. Overall, these findings describe a new role for PDIM during Mtb infection and support the model that PGE_2 and type I IFNs negatively regulate one another in Mtb-infected macrophages in a cell intrinsic manner.

In addition to PDIM, Mtb-infected macrophages require the presence of ESAT-6 for PGE_2 production as Mtb mutants lacking either virulence factor are unable to induce PGE_2 during infection. It is known that ESAT-6 and PDIM are both essential for Mtb to escape the phagosome and access the host cytosol [3-6, 11]. Therefore, it is possible that Mtb must be present in the cytosol to induce PGE_2 production and PDIM-deficient mutants do not induce PGE_2 because they are unable to escape the phagosome. Interestingly, PGE_2 is also detected when macrophages are treated with C18 reverse phase beads coated with wild type or mas comp lipids. As proteins are stripped away during the lipid extraction process, this would imply that PDIM alone is necessary for macrophage PGE_2 production. The amount of PDIM present on the beads remains to be assessed, so it is possible that the beads are overloaded with PDIM and when in excess this lipid can rupture the phagosome in the absence of ESAT-6. Alternatively, the beads themselves may have the ability to directly lyse membranes due to their hydrophobic surface (saturated 18-Carbon acyl group). This could release PDIM into the cytosol where the lipid is sensed and triggers PGE_2 production. Both possibilities will need to be addressed in future work.

Historically, PGE_2 production in response to Mtb infection has been linked directly to IL-1β [8]. Unexpectedly, we observed that PDIM-dependent PGE_2 production in infected macrophages occurs independently of inflammasome activation and IL-1β signaling through IL-1R. In contrast, TLR signaling is required as $MYD88^{-/-}$ macrophages produce no PGE_2 in response to Mtb. This suggests that TLR activation by Mtb can lead to PGE_2 synthesis through an unidentified pathway. While the players

in this pathway remain to elucidated, our data suggests that cathepsin B may be involved as it is required for PGE_2 production in macrophages.

While the data shows a strong link between PDIM and PGE_2 production early in Mtb infection, the overarching role PGE_2 plays during infection remains unclear. The presence of PGE_2 is thought to drive apoptotic death of infected macrophages facilitating elimination of Mtb [9]. Further experiments will need to be conducted to address the effect PDIM-dependent PGE_2 production has on the fate of the host cell and if this process is important at later stages of infection.

EXPERIMENTAL PROCEDURES

Strains and growth conditions

The *E coli* strains Top10 (Invitrogen) and T7 Express (New England Biolabs) were used for molecular cloning. *E. coli* strains were grown in LB medium and transformants were selected on LB plates containing kanamycin (25 μg ml^{-1}), zeocin (25 μg ml^{-1}) or hygromycin (100 μg ml^{-1}). Mtb Erdman strains were cultivated in 7H9 medium (BD Biosciences) containing OADC supplement (BD Biosciences) unless otherwise noted. The strain $mas^{Pro1223delC}$ was obtained via screening wild type Erdman colonies for point mutations in PDIM synthesis genes; it was found that this strain contains a single CG base pair deletion 3669 bp into *mas/Rv2940c* causing a frameshift and a stop codon to truncate the gene 22 bp downstream of the deletion. Complementation was achieved through introduction of a full-length *mas/Rv2940c* gene under control of its native promoter in a pMV306 integrating plasmid. To create the Δ*ESAT-6* mutant strain, the entire *ESAT-6/Rv3875* open reading frame was replaced with a hygromycin cassette via allelic exchange and confirmed with sequencing [28]. Mutant colonies were screened for presence and absence of PDIM. These strains were complemented through introduction of *CFP10/Rv3874* and *ESAT-6/Rv3875* under control of the hsp60 promoter in a pMV306 integrating plasmid. All complemented strains were checked for the presence or absence of PDIM.

Thin-layer chromatography

Bacteria were growth to mid-log phase and then labeled for 24 hours with ^{14}C-propionate at 37˚C. Following labeling cells were harvested in chloroform:methanol (2:1 v/v) and total lipids were extracted as described [29]. Where applicable surface

lipids were removed with hexane prior to chloroform:methanol extraction as described [30]. Lipids were resolved with TLC in petroleum ether:ethyl acetate (98:2 v/v) solvent system before visualizing with a Typhoon Imager (Amersham).

Lipid extraction and bead coating

Bacteria were growth to mid-log phase then harvested in 2:1 chloroform:methanol (v/v) and total lipids were extracted as described [29]. To coat beads with Mtb lipids, 4 mg of reverse phase chromatography beads (C18, 3 micron) were mixed with 2.0 mg of total lipids were mixed in 2:1 chloroform:methanol (v/v). The lipids and beads were dried under a stream of nitrogen gas. Lipid-coated beads were re-suspended in PBS with sonication, washed thrice with cold PBS at 4˚C, and re-suspended in 1 ml cold PBS. Concentration of lipid coated beads was quantified with a hemocytometer.

BMMO isolation, infection, and sample harvest

Macrophages were derived from the bone marrow from femurs of BALB/c or C57BL/6 mice (Jackson), 6-8 weeks of age. The bone-marrow-derived macrophages were seeded into T-25 tissue culture flasks (8×10^6 cells per flask) and infected with Mtb at a MOI of 1:1 or treated with lipid-coated C18 beads at a MOI of 2:1. For each experiment 3 biological replicates of bone-marrow-derived macrophages used. When applicable, macrophages were treated with DMSO, 20 μM MCC950, or 20 μM CA-074 at the time of treatment with lipid-coated C18 beads. At 24-hours and/or 48-hours post-infection supernatants were collected for analysis via ELISA or mixed 1:1 with methanol for mass-spectrometry analysis. Immediately after infection and 24-hours and/or 48-hours post-infection infected macrophages were lysed with 0.05% sodium

dodecyl sulfate and plated on 7H10 OADC agar to quantify bacterial burden. CFU were quantified after 3–4 weeks incubation at 37°C.

Enzyme-linked immunosorbent assays

PGE_2 and IL-1β from macrophage supernatants and mouse lung homogenates were quantified using the Cayman Chemical Prostaglandin E_2 ELISA kit (Item No. 514010) and the R&D Systems Mouse IL-1 beta/IL-1F2 Quantikine ELISA Kit (Catalog #: MLB00C), respectively. All samples were assayed in two dilutions and in duplicate following kit instructions. Absorbances were measured using an Envision plate reader.

Quantitative Mass-spectrometry

Mass-spectrometry of eicosanoids from the supernatants of infected BMMΦ was performed by Cayman Chemical. All internal and calibration standards used are listed below on Table 1. To prepare the calibration curves, a mixture of the 19 calibration standards listed below was prepared in ethanol at a concentration of 1 μg/mL each, then diluted to 270 ng/mL in water:acetonitrile 1:1 (v/v). This calibration sample (Cal 10) was further diluted in a series of nine 1/3 dilutions in water:acetonitrile 1:1 (v/v) down to a concentration of 0.0137 ng/mL (Cal 1). Quality control (QC) samples were prepared by diluting the 1 μg/mL mixture of calibration standards in water:acetonitrile 1:1 (v/v) to concentrations of 200 ng/mL, 20 ng/mL, 2 ng/mL, and 0.2 ng/mL. A separate curve and QC set was prepared for 12-HHTrE and 18-HEPE due to poor performance of these analytes in test curves run before analysis. These standards were prepared following the same protocol as the other standards and extracted alongside the main calibrator and QC samples. The internal standard mixture

was prepared by mixing the deuterated standards listed above in methanol to a concentration of 10 ng/mL each.

Mouse macrophage cell culture media samples were received frozen on dry ice and placed in -80 °C storage until use. After thawing on wet ice, 450 µL from each mouse macrophage cell culture media sample were transferred to individual 1.5 mL Eppendorf tubes. To each sample, 50 µL internal standard mixture and 50 µL water:acetonitrile 1:1 (v/v) were added. Likewise, 50 µL from each calibrator and QC sample were transferred to individual 1.5 mL Eppendorf tubes, before addition of 50 µL internal standard mixture and 450 µL PBS. Samples were mixed thoroughly and placed at -80 °C overnight to improve extraction. After thawing on wet ice, the samples were mixed well and centrifuged for 15 min at 16000 x *g*. After centrifugation, 500 µL of the supernatants were transferred to a 1 mL 96-well plate, diluted with 200 µL water, and mixed thoroughly before being transferred to a 96-well solid-phase extraction plate (Strata-X 33 µm, Polymeric Reversed Phase, 10 mg, Phenomenex) previously equilibrated with 2 mL methanol followed by 2 mL water. Using a nitrogen gas-driven positive-pressure manifold from Biotage, the extraction plate was washed with 1 mL water and 1 mL water:methanol 9:1 (v/v), then eluted with 1 mL methanol into a 96-well glass-insert plate (U-2D plate system, MicroSolv Technology Corp). The eluent was evaporated under a gentle stream of nitrogen using a ZipVap Evaporator. After the extracts were resuspended in 100 µL water:acetonitrile 60:40 (v/v), the glass-insert plate was fitted with a silicone plate mat and placed in the LC-MS/MS autosampler. An aliquot of 10 µL was injected into the LC-MS/MS

system for analysis. The details and instrument parameters used are listed on the accompanying Excel data file.

The lower limit of quantitation (LLQ) for each analyte was determined using the data of the calibration curves. A signal/noise minimum ratio of 5 was established and applied during peak selection and review. The chromatographic profile of the ion count for each *m/z* transition was monitored, and the area under the peak (ion count *vs* elution time) integrated using commercial software (MultiQuant, Sciex). The area ratios of each analyte detected were interpolated in the calibration curve for the corresponding authentic standard, or in some cases for a structurally similar surrogate standard as listed on the accompanying Excel file. Calculations of the total amount of each eicosanoid present in each sample were performed using MultiQuant software.

Internal Standards		Calibration Standards	
Analyte	**Cayman Catalog Number**	**Analyte**	**Cayman Catalog Number**
PGE_2-d_4	10007273	**PGE_2**	10007211
TXB_2-d_4	319030	**TXB_2**	10007237
5(S)-HETE-d_8	334230	**5(S)-HETE**	10007243
LTB_4-d_4	29629	**LTB_4**	10007240
LTD_4-d_5	25370	**LTD_4**	25369
LXA_4-d_5	24936	**LXA_4**	10007271
14(15)-EET-d_{11}	26970	**14(15)-EET**	10007263
14(15)-DiHET-d_{11}	25032	**14(15)-DiHET**	10007267
9(S)-HODE-d_4	25368	**9(S)-HODE**	23569
RvE1-d_4	10009854	**RvE1**	10007848
RvD1-d_5	11182	**RvD1**	25905
		6-keto $PGF_{1\alpha}$	10007219
		$PGF_{2\alpha}$	10007221
		PGJ_2	18500
		12-HHTrE	34590
		LTC_4	10007241
		20-HETE	10007269
		17-HDHA	10007223
		18-HEPE	23567

Table 1. Deuterated internal standards and calibration standards used in oxylipin analysis for this project.

Mouse infection studies

Animal work was approved by Cornell University IACUC (protocol number 2013-0030). All protocols conform to the USDA Animal Welfare Act, institutional policies on the care and humane treatment of animals, and other applicable laws and regulations. Six to eight-week-old female BALB/c wild type mice Jackson Laboratories were infected with 1000 CFU of Mtb strains via an aerosolization. At sacrifice, the lungs were removed. The lungs were homogenized in PBS 0.05% Tween-80 and 100 μM indomethacin (COX-2 inhibitor). and plated on 7H10 OADC agar to determine bacterial burden or used for analysis via ELISA. CFU were quantified after 3–4 weeks incubation at 37°C.

REFERENCES

1. *Global tuberculosis report 2022. Geneva: World Health organization; 2022. licence: CC BY-NC-SA 3.0 IGO.*

2. Guinn, K.M., et al., *Individual RD1-region genes are required for export of ESAT-6/CFP-10 and for virulence of Mycobacterium tuberculosis.* Mol Microbiol, 2004. **51**(2): p. 359-70.

3. Simeone, R., et al., *Phagosomal rupture by Mycobacterium tuberculosis results in toxicity and host cell death.* PLoS Pathog, 2012. **8**(2): p. e1002507.

4. Augenstreich, J., et al., *ESX-1 and phthiocerol dimycocerosates of Mycobacterium tuberculosis act in concert to cause phagosomal rupture and host cell apoptosis.* Cell Microbiol, 2017. **19**(7).

5. van der Wel, N., et al., *M. tuberculosis and M. leprae translocate from the phagolysosome to the cytosol in myeloid cells.* Cell, 2007. **129**(7): p. 1287-98.

6. Houben, D., et al., *ESX-1-mediated translocation to the cytosol controls virulence of mycobacteria.* Cell Microbiol, 2012. **14**(8): p. 1287-98.

7. Manzanillo, P.S., et al., *Mycobacterium tuberculosis activates the DNA-dependent cytosolic surveillance pathway within macrophages.* Cell Host Microbe, 2012. **11**(5): p. 469-80.

8. Mayer-Barber, K.D., et al., *Host-directed therapy of tuberculosis based on interleukin-1 and type I interferon crosstalk.* Nature, 2014. **511**(7507): p. 99-103.

9. Chen, M., et al., *Lipid mediators in innate immunity against tuberculosis: opposing roles of PGE2 and LXA4 in the induction of macrophage death.* J Exp Med, 2008. **205**(12): p. 2791-801.

10. Rens, C., et al., *Roles for phthiocerol dimycocerosate lipids in Mycobacterium tuberculosis pathogenesis.* Microbiology (Reading), 2021. **167**(3).

11. Barczak, A.K., et al., *Systematic, multiparametric analysis of Mycobacterium tuberculosis intracellular infection offers insight into coordinated virulence.* 2017. **13**(5): p. e1006363.

12. Quigley, J., et al., *The Cell Wall Lipid PDIM Contributes to Phagosomal Escape and Host Cell Exit of Mycobacterium tuberculosis.* mBio, 2017. **8**(2).

13. Lerner, T.R., et al., *Phthiocerol dimycocerosates promote access to the cytosol and intracellular burden of Mycobacterium tuberculosis in lymphatic endothelial cells.* BMC Biol, 2018. **16**(1): p. 1.

14. Peng, X., et al., *Characterization of differential pore-forming activities of ESAT-6 proteins from Mycobacterium tuberculosis and Mycobacterium smegmatis.* FEBS Lett, 2016. **590**(4): p. 509-19.

15. Augenstreich, J., et al., *Phthiocerol Dimycocerosates From Mycobacterium tuberculosis Increase the Membrane Activity of Bacterial Effectors and Host Receptors.* Front Cell Infect Microbiol, 2020. **10**: p. 420.

16. Berry, M.P., et al., *An interferon-inducible neutrophil-driven blood transcriptional signature in human tuberculosis.* Nature, 2010. **466**(7309): p. 973-7.

17. McDougal, C.E., et al., *Phagocytes produce prostaglandin E2 in response to cytosolic Listeria monocytogenes.* PLoS Pathog, 2021. **17**(9): p. e1009493.

18. VanderVen, B.C., et al., *Development of a novel, cell-based chemical screen to identify inhibitors of intraphagosomal lipolysis in macrophages.* Cytometry Part A, 2010. **77A**(8): p. 751-760.

19. Goren, M.B., O. Brokl, and W.B. Schaefer, *Lipids of putative relevance to virulence in Mycobacterium tuberculosis: phthiocerol dimycocerosate and the attenuation indicator lipid.* Infect Immun, 1974. **9**(1): p. 150-8.

20. Camacho, L.R., et al., *Identification of a virulence gene cluster of Mycobacterium tuberculosis by signature-tagged transposon mutagenesis.* Mol Microbiol, 1999. **34**(2): p. 257-67.

21. Cox, J.S., et al., *Complex lipid determines tissue-specific replication of Mycobacterium tuberculosis in mice.* Nature, 1999. **402**(6757): p. 79-83.

22. Kleinnijenhuis, J., et al., *Transcriptional and inflammasome-mediated pathways for the induction of IL-1beta production by Mycobacterium tuberculosis.* Eur J Immunol, 2009. **39**(7): p. 1914-22.

23. Silverio, D., et al., *Advances on the Role and Applications of Interleukin-1 in Tuberculosis.* mBio, 2021. **12**(6): p. e0313421.

24. Rocca, B. and G.A. FitzGerald, *Cyclooxygenases and prostaglandins: shaping up the immune response.* Int Immunopharmacol, 2002. **2**(5): p. 603-30.

25. Sheppe, A.E.F. and M.J. Edelmann, *Roles of Eicosanoids in Regulating Inflammation and Neutrophil Migration as an Innate Host Response to Bacterial Infections.* Infect Immun, 2021. **89**(8): p. e0009521.

26. Chevriaux, A., et al., *Cathepsin B Is Required for NLRP3 Inflammasome Activation in Macrophages, Through NLRP3 Interaction.* Front Cell Dev Biol, 2020. **8**: p. 167.

27. Mayer-Barber, K.D., et al., *Innate and adaptive interferons suppress IL-1alpha and IL-1beta production by distinct pulmonary myeloid subsets during Mycobacterium tuberculosis infection.* Immunity, 2011. **35**(6): p. 1023-34.

28. Mann, F.M., B.C. VanderVen, and R.J. Peters, *Magnesium depletion triggers production of an immune modulating diterpenoid in Mycobacterium tuberculosis.* Mol Microbiol, 2011. **79**(6): p. 1594-601.

29. Bligh, E. and W. Dyer, *A rapid method of total lipid extraction and purification.* Can J Biochem Physiol, 1959(37): p. 911-917.

30. Jain, M. and J.S. Cox, *Interaction between polyketide synthase and transporter suggests coupled synthesis and export of virulence lipid in M. tuberculosis.* PLoS Pathog, 2005. **1**(1): p. e2.

CHAPTER 4

Summary and Future Directions

Mce-Mediated Lipid Assimilation in Mtb

The Mtb genome contains four closely related *mce* operons (termed *mce1-4*) which encode permease and substrate binding subunits for four separate, substrate specific transporters. It is established that Mce1 imports fatty acids and Mce4 imports cholesterol while the substrates of Mce2 and Mce3 remain unknown [1, 2]. Additionally, transport activity of Mce1 and Mce4 require proteins encoded elsewhere in the genome, supporting the model where the substrate specific Mce transporters each require shared proteins to regulate and/or facilitate transport activity [1, 3]. One protein essential to both Mce1- and Mce4-mediated lipid uptake is MceG, a predicted ATPase. This work sought to confirm the putative ATPase activity of MceG and further characterize its function in lipid import. We determined that a defined mutant lacking MceG is defective in fatty acid and cholesterol import and has an *in vivo* fitness defect. Additionally, components of the Mce1 transporter are degraded in Mtb strains lacking MceG or MceG enzymatic activity. Together this data suggests that enzymatic activity of MceG is required for fatty acid and cholesterol import as well as stability of the Mce1 complex.

These findings raise the question of how Mtb regulates Mce1- and Mce4-mediated transport. In bacteria that express catalytically inactive MceG, the substrate binding subunits of Mce1 are almost entirely degraded while transcription and translation of Mce1 components is unaltered. It is possible that an unknown protease in the Mtb cell wall is responsible for dismantling Mce1 in the absence of MceG. To identify this putative protease, one could delete candidate proteases in the ΔMceG mutant background and evaluate if the Mce1 proteins are stabilized. Additionally, MceG

contains a C-terminal regulatory domain that is essential for fatty acid and cholesterol utilization (data not shown) [4]. It is possible that proteins or metabolites bind to the C-terminal region of MceG and cause conformational changes affecting enzymatic activity, but further experiments will be needed to determine if MceG is regulated in this manner. Recent work has established that the protein, Mce1N, negatively regulates Mce1 function in *M. smegmatis* by preventing MceG from binding to the YrbE1B permease [5]. Mtb contains a homolog of Mce1N and it is possible that Mce1N also negatively regulates fatty acid uptake Mtb. In what environmental conditions Mtb would employ Mce1N to inhibit MceG binding and whether Mce1N regulates the other Mce complexes remains to be elucidated.

Through our proteomics approach we sought to not only determine the levels of Mce proteins present in the ΔMceG mutant, but also identify other proteins possibly associated with the Mce complexes. In addition to Mce1 and Mce4 proteins, three other proteins were found to be underrepresented when MceG is absent. One of the proteins, Rv2536, has since been confirmed to associate with Mce1 and was named LucB [6]. The function of LucB is unknown, but this transmembrane protein has a c-terminal tail that extends into the cytoplasm which may play a regulatory or structural role. The other two proteins that were underrepresented in the ΔMceG mutant analysis were Rv2190/RipC and Rv0062/CelA1 which have peptidoglycan hydrolase activity and cellulase activity, respectively [7-10]. Our future work will determine whether Rv2190/RipC or Rv0062/CelA1 are involved in the turnover or function of the Mce1 and Mce4 transporters. Lastly, Rv1999c was the only protein found to be overrepresented in the ΔMceG mutant. The function of Rv1999c is unknown but as it

is predicted to be an integral membrane transporter, we hypothesize that it may function to import nutrients in the ΔMceG mutant to compensate for the lack of Mce1- and Mce4-mediated lipid utilization. Ongoing experiments are addressing possible transport activity and substrates for Rv1999c.

The full range of lipids that Mtb is capable of utilizing has not been defined. Theoretically, Mtb has access to more lipid nutrients than cholesterol and C16 and C18 fatty acids throughout the course of infection. During the intracellular phase of its lifecycle, Mtb likely has access to the cholesterol, cholesteryl-ester, and triacylglycerol that accumulate in macrophage lipid droplets [11-13]. While living extracellularly in the necrotic center of granulomas, Mtb is in an environment with significant levels of cholesterol, cholesteryl-ester, triacylglycerol, and lactosylceramide [14-16]. Additionally, lipid droplets function as sites of eicosanoid biosynthesis and contain arachidonic acid and its metabolic products [17]. The range of host lipids may be further defined by using radiolabeled candidate substrates to test Mce-1 dependent import. Using this method, we determined that Mtb metabolizes and assimilates arachidonic acid in an Mce-1 dependent manner (Figure 4.1A and 4.1B). What metabolic enzymes Mtb uses to metabolize polyunsaturated fatty acids and whether levels of arachidonic acid import by Mtb are significant enough *in vivo* to perturb host pools of eicosanoids remains to be determined. Uncovering the range of lipids that Mce complexes import may provide more insight into how substrate specificity is determined as well as further characterize aspects of Mtb survival during infection.

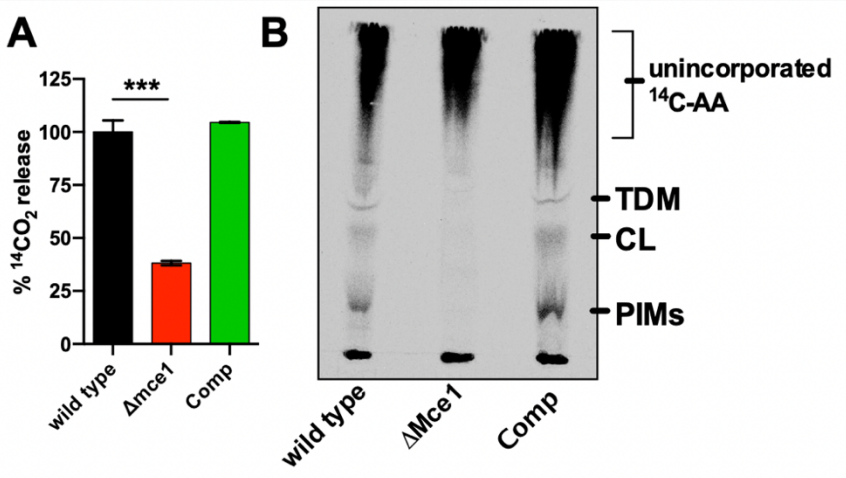

Figure 4.1 Mtb imports, metabolizes, and assimilates arachidonic acid (AA) in an Mce1-dependent manner. (A) Metabolic oxidation of ^{14}C-AA. **(B)** TLC autoradiogram of lipid extracts isolated from Mtb following pulse labeling with ^{14}C-AA. Equal counts of Mtb lipids (40k CPM) were resolved in a solvent system for polar lipids. Cardiolipin (CL), trehalose dimycolate (TDM), and phosphatidylinositol mannosides (PIMs). Metabolism data are from 2 independent experiments with 3 technical replicates per group. Data are means +/- SD. ***$p<0.005$ (Student's t test).

Understanding how Mtb assimilates nutrients will expand what is currently limited knowledge about how transporters with Mce-domain containing proteins function. Accumulating evidence shows that Mce domain-containing proteins are generally involved in the transport of hydrophobic molecules, and this function is consistent across a wide range of organisms. In addition to Mycobacteria, Mce domain containing proteins are found broadly across gram-negative bacteria and are even utilized in chloroplasts of eukaryotic cells [18-23]. Uncovering structural components that define substrate specificity and determining the range of lipid species that interact with Mtb's Mce proteins would add to the body of literature regarding the transport of hydrophobic molecules across double membranes as well as inform studies surrounding Mce proteins in other organisms.

In addition to facilitating the translocation of lipids, the *mce* operons have been shown to play a role in virulence. Mutations in the *mce2*, *mce3*, or *mce4* operons result in attenuation of Mtb in a mouse model of infection [2, 24-27]. Therefore, novel therapeutics that inhibit lipid utilization by the bacteria have potential value and more information relating to lipid utilization would better equip the field in their endeavor to find ways to perturb Mtb's persistent life cycle. More specifically, bridging the gaps in knowledge regarding the range of host lipids utilized by Mtb and mechanistic details surrounding the Mce transport complexes would potentially unveil bottlenecks in these pathways that could be exploited by novel therapeutics.

PDIM-dependent PGE_2 production during Mtb infection

Not only do the lipids that make up the cell envelope of Mtb provide a formidable hydrophobicity barrier, but they are also crucial virulence factors for Mtb that interact with the host immune system at every step of Mtb's lifecycle. Of particular importance is the lipid phthiocerol dimycocerosate (PDIM), which is incorporated into the outer leaflet of the Mtb outer membrane [28]. PDIM is a critical virulence factor for Mtb as it is always present in clinical isolates recovered from humans and mutant lab strains without the ability to synthesize PDIM are attenuated early in infection [29-31].

PDIM has been implicated in many different aspects of Mtb pathogenesis including resisting acidification of the macrophage phagosome, preventing induction of pro-inflammatory cytokines such TNF-α and IL-6 early in infection, preventing detection by TLRs by masking pathogen-associated molecular patterns (PAMPs), and

inhibiting recruitment of NO producing macrophages [32-36]. More recently, evidence has accumulated to support a role for PDIM in phagosome permeabilization and bacterial escape into the host cytosol, in conjunction with the secreted protein ESAT-6 [37-39]. PDIM- and ESAT-6-dependent phagosomal escape induces production of macrophage type I interferons (IFNs) and host cell death implying that this process may facilitate bacterial spread [37-43].

Our studies reveal a previously unknown role for PDIM in the induction of PGE_2 production during early stages of infection. Mtb lacking PDIM fail to induce PGE_2 in macrophages and in mice and is defecting in phagosomal rupture. We propose that PDIM and ESAT-6 facilitate deposition of Mtb into the host cytosol where PDIM is sensed by host cells thereby triggering a signaling pathway that results in biosynthesis of PGE_2. Whether it is PDIM itself that is being sensed by the host cell or another Mtb PAMP will need to be investigated in future studies.

Although in previous studies IL-1β signaling has been shown to trigger PGE_2 production in Mtb infected macrophages, we found that IL-1β signaling is not required for PDIM-dependent PGE_2 production in the tested conditions [44]. However, activation of toll-like receptors (TLRs) and cathepsin B is required. This implies that PGE_2 is induced in a PDIM-dependent manner through an unknown pathway. To identify other factors required for this pathway, we propose conducting RNA-seq analysis comparing the transcriptional profile of macrophages infected with PDIM-positive and PDIM-deficient strains of Mtb. We expect to see differential expression of COX-2, the enzyme necessary for PGE_2 biosynthesis, and it is possible there will be other macrophage genes expressed in a PDIM-dependent manner. Additionally, other

factors required for PDIM-dependent PGE_2 production could be identified by conducting a genetic screen using a CRISPR/cas9 macrophage library and a fluorescent antibody specific for COX-2. By infecting the macrophage library with PDIM-positive Mtb, factors required for PGE_2 induction could be identified through isolation of infected macrophages that are negative for COX-2 staining and therefore do not produce PGE_2 in response to PDIM. Any candidates from either approach could then be validated through the use of inhibitors or knockout mouse strains.

The role PDIM plays in perturbing the host immune response has been extensively studied so it is curious that this is the first observation made linking PDIM to PGE_2 production. There are various laboratory strains of Mtb that are used across laboratories and across time. For these studies, we used Mtb Erdman, but historically H37Rv has been used widely by the field. When testing different strains of Mtb in our assays, we found that both wild type Erdman and wild type H37Rv produce PDIM, but compared to wild type Erdman, wild type H37Rv does not efficiently induce PGE_2 in macrophages (Figure 4.2A and 4.B). While strains of Mtb from Lineage 8 have been shown to produce modified versions of PDIM, Erdman and H37Rv are from Lineage 4 and therefore due to their genetic similarity have been assumed to produce structurally similar versions of unmodified PDIM [45, 46]. Even though these strains were first isolated from human patients, it is possible that as laboratory strains they have diverged through extensive passaging. Further studies will need to be conducted to investigate possible structural differences between the PDIM produced by Erdman and H37Rv. Additional testing of Mtb isolates from other lineages could also identify

possible links between specific structural characteristics of PDIM and its ability to induce PGE_2 during infection.

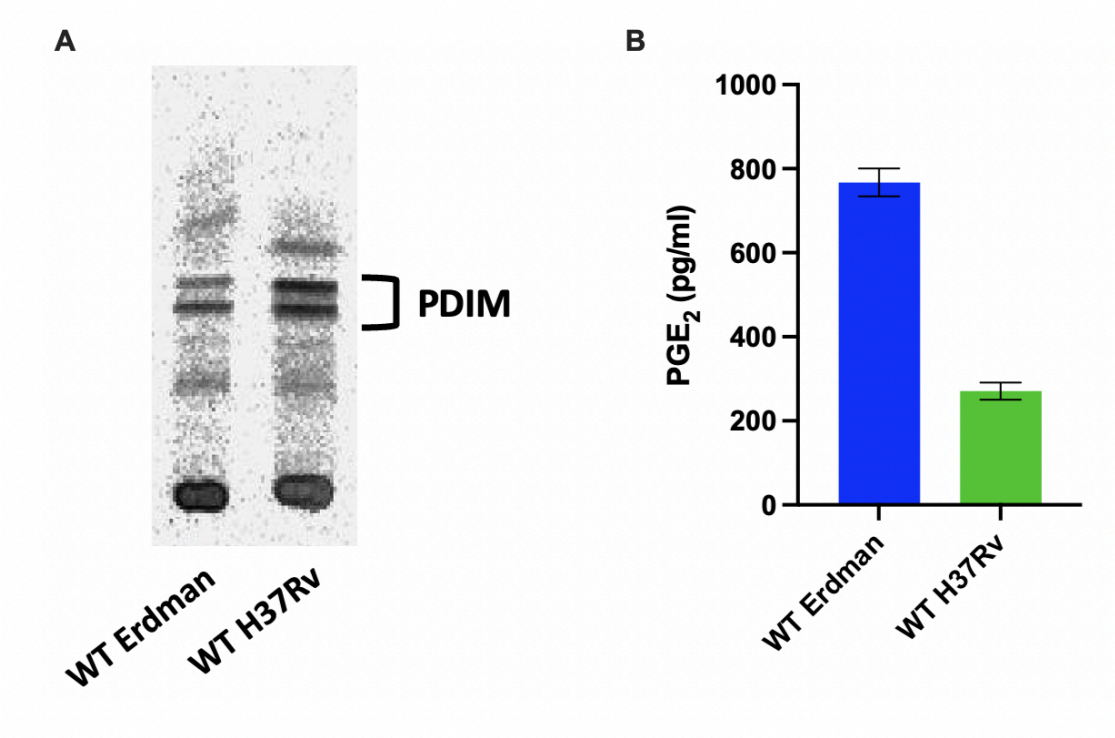

Figure 4.2 Phenotypic differences in PGE_2 production in macrophages infected with different lab strains of Mtb. (A) TLC autoradiogram of total lipid extracts isolated from Mtb following labeling with ^{14}C-propionate. Equal counts of Mtb lipids (20K CPM) were resolved in a petroleum ether:ethyl acetate (98:2 v/v). Bands corresponding to PDIM are labeled. **(B)** PGE_2 levels secreted by BALB/c BMMΦ infected with wild type Erdman and wild type H37Rv Mtb for 24-hours were quantified by ELISA.

Lastly, our studies implicate PDIM and ESAT-6 in macrophage PGE_2 production, but the effect that this interaction has on the fate of Mtb during infection remains unclear. PDIM- and ESAT-6-dependent phagosomal escape has been shown to induce production of type I IFNs possibly leading to necrosis of the host cell and bacterial dissemination [38, 40, 44]. In contrast, PGE_2 production during Mtb infection

has been associated with apoptosis of host cells and bacterial elimination [47]. It would be of value to assess host cell death phenotypes in PDIM-positive and PDIM-negative infected macrophages to uncover more information regarding the relationship between PDIM-dependent PGE_2 production and bacterial fate during infection. Overall, our studies have further defined the role PDIM plays in Mtb virulence, but the mechanisms underlying PGE_2 production during Mtb infection remain to be determined.

REFERENCES

1. Nazarova, E.V., et al., *Rv3723/LucA coordinates fatty acid and cholesterol uptake in Mycobacterium tuberculosis.* 2017. **6**.

2. Pandey, A.K. and C.M. Sassetti, *Mycobacterial persistence requires the utilization of host cholesterol.* Proceedings of the National Academy of Sciences, 2008. **105**(11): p. 4376-4380.

3. Perkowski, E.F., et al., *An orphaned Mce-associated membrane protein of Mycobacterium tuberculosis is a virulence factor that stabilizes Mce transporters.* Mol Microbiol, 2016. **100**(1): p. 90-107.

4. Garcia-Fernandez, J., et al., *Unraveling the pleiotropic role of the MceG ATPase in Mycobacterium smegmatis.* Environ Microbiol, 2017.

5. Chen, Y., Y. Wang, and S.-S. Chng, *A conserved membrane protein negatively regulates Mce1 complexes in mycobacteria.* bioRxiv, 2023: p. 2022.06.08.495402.

6. Chen, J., et al., *Structure of an endogenous mycobacterial MCE lipid transporter.* Res Sq, 2023.

7. Varrot, A., et al., *Mycobacterium tuberculosis strains possess functional cellulases.* J Biol Chem, 2005. **280**(21): p. 20181-4.

8. Trivedi, A., et al., *Thiol reductive stress induces cellulose-anchored biofilm formation in Mycobacterium tuberculosis.* Nat Commun, 2016. **7**: p. 11392.

9. Anantharaman, V. and L. Aravind, *Evolutionary history, structural features and biochemical diversity of the NlpC/P60 superfamily of enzymes.* Genome Biol, 2003. **4**(2): p. R11.

10. Mavrici, D., et al., *Mycobacterium tuberculosis FtsX extracellular domain activates the peptidoglycan hydrolase, RipC.* Proc Natl Acad Sci U S A, 2014. **111**(22): p. 8037-42.

11. Russell, D.G., et al., *Foamy macrophages and the progression of the human tuberculosis granuloma.* Nat Immunol, 2009. **10**(9): p. 943-8.

12. Peyron, P., et al., *Foamy macrophages from tuberculous patients' granulomas constitute a nutrient-rich reservoir for M. tuberculosis persistence.* PLoS Pathog, 2008. **4**(11): p. e1000204.

13. Guo, Y., et al., *Lipid droplets at a glance.* J Cell Sci, 2009. **122**(Pt 6): p. 749-52.

14. Hunter, R.L., C. Jagannath, and J.K. Actor, *Pathology of postprimary tuberculosis in humans and mice: contradiction of long-held beliefs.* Tuberculosis (Edinb), 2007. **87**(4): p. 267-78.

15. Martin, C.J., A.F. Carey, and S.M. Fortune, *A bug's life in the granuloma.* Semin Immunopathol, 2016. **38**(2): p. 213-20.

16. Kim, M.J., et al., *Caseation of human tuberculosis granulomas correlates with elevated host lipid metabolism.* EMBO Mol Med, 2010. **2**(7): p. 258-74.

17. Da'Avila, H., et al., *Mycobacterium bovis Bacillus Calmette-Guerin Induces TLR2-Mediated Formation of Lipid Bodies: Intracellular Domains for Eicosanoid Synthesis In Vivo.* The Journal of Immunology, 2006. **176**(5): p. 3087-3097.

18. Casali, N. and L.W. Riley, *A phylogenomic analysis of the Actinomycetales mce operons.* BMC Genomics, 2007. **8**: p. 60.

19. Awai, K., et al., *A phosphatidic acid-binding protein of the chloroplast inner envelope membrane involved in lipid trafficking.* Proc Natl Acad Sci U S A, 2006. **103**(28): p. 10817-22.

20. Krachler, A.M., H. Ham, and K. Orth, *Outer membrane adhesion factor multivalent adhesion molecule 7 initiates host cell binding during infection by gram-negative pathogens.* Proc Natl Acad Sci U S A, 2011. **108**(28): p. 11614-9.

21. Lu, B. and C. Benning, *A 25-amino acid sequence of the Arabidopsis TGD2 protein is sufficient for specific binding of phosphatidic acid.* J Biol Chem, 2009. **284**(26): p. 17420-7.

22. Isom, G.L., et al., *MCE domain proteins: conserved inner membrane lipid-binding proteins required for outer membrane homeostasis.* Sci Rep, 2017. **7**(1): p. 8608.

23. Thong, S., et al., *Defining key roles for auxiliary proteins in an ABC transporter that maintains bacterial outer membrane lipid asymmetry.* 2016. **5**.

24. Sassetti, C.M. and E.J. Rubin, *Genetic requirements for mycobacterial survival during infection.* Proceedings of the National Academy of Sciences of the United States of America, 2003. **100**(22): p. 12989-12994.

25. Gioffre, A., et al., *Mutation in mce operons attenuates Mycobacterium tuberculosis virulence.* Microbes Infect, 2005. **7**(3): p. 325-34.

26. Marjanovic, O., et al., *Mce2 operon mutant strain of Mycobacterium tuberculosis is attenuated in C57BL/6 mice.* Tuberculosis (Edinb), 2010. **90**(1): p. 50-6.

27. Senaratne, R.H., et al., *Mycobacterium tuberculosis strains disrupted in mce3 and mce4 operons are attenuated in mice.* J Med Microbiol, 2008. **57**(Pt 2): p. 164-70.

28. Jackson, M., *The mycobacterial cell envelope-lipids.* Cold Spring Harb Perspect Med, 2014. **4**(10).

29. Camacho, L.R., et al., *Identification of a virulence gene cluster of Mycobacterium tuberculosis by signature-tagged transposon mutagenesis.* Mol Microbiol, 1999. **34**(2): p. 257-67.

30. Cox, J.S., et al., *Complex lipid determines tissue-specific replication of Mycobacterium tuberculosis in mice.* Nature, 1999. **402**(6757): p. 79-83.

31. Goren, M.B., O. Brokl, and W.B. Schaefer, *Lipids of putative relevance to virulence in Mycobacterium tuberculosis: phthiocerol dimycocerosate and the attenuation indicator lipid.* Infect Immun, 1974. **9**(1): p. 150-8.

32. Rousseau, C., et al., *Production of phthiocerol dimycocerosates protects Mycobacterium tuberculosis from the cidal activity of reactive nitrogen intermediates produced by macrophages and modulates the early immune response to infection.* Cell Microbiol, 2004. **6**(3): p. 277-87.

33. Astarie-Dequeker, C., et al., *Phthiocerol dimycocerosates of M. tuberculosis participate in macrophage invasion by inducing changes in the organization of plasma membrane lipids.* PLoS Pathog, 2009. **5**(2): p. e1000289.

34. Murry, J.P., et al., *Phthiocerol dimycocerosate transport is required for resisting interferon-gamma-independent immunity.* J Infect Dis, 2009. **200**(5): p. 774-82.

35. Kirksey, M.A., et al., *Spontaneous phthiocerol dimycocerosate-deficient variants of Mycobacterium tuberculosis are susceptible to gamma interferon-mediated immunity.* Infect Immun, 2011. **79**(7): p. 2829-38.

36. Cambier, C.J., et al., *Mycobacteria manipulate macrophage recruitment through coordinated use of membrane lipids.* Nature, 2014. **505**(7482): p. 218-22.

37. Augenstreich, J., et al., *ESX-1 and phthiocerol dimycocerosates of Mycobacterium tuberculosis act in concert to cause phagosomal rupture and host cell apoptosis.* Cell Microbiol, 2017. **19**(7).

38. Barczak, A.K., et al., *Systematic, multiparametric analysis of Mycobacterium tuberculosis intracellular infection offers insight into coordinated virulence.* 2017. **13**(5): p. e1006363.

39. Quigley, J., et al., *The Cell Wall Lipid PDIM Contributes to Phagosomal Escape and Host Cell Exit of Mycobacterium tuberculosis.* mBio, 2017. **8**(2).

40. Manzanillo, P.S., et al., *Mycobacterium tuberculosis activates the DNA-dependent cytosolic surveillance pathway within macrophages.* Cell Host Microbe, 2012. **11**(5): p. 469-80.

41. Guinn, K.M., et al., *Individual RD1-region genes are required for export of ESAT-6/CFP-10 and for virulence of Mycobacterium tuberculosis.* Mol Microbiol, 2004. **51**(2): p. 359-70.

42. van der Wel, N., et al., *M. tuberculosis and M. leprae translocate from the phagolysosome to the cytosol in myeloid cells.* Cell, 2007. **129**(7): p. 1287-98.

43. Stanley, S.A., et al., *The Type I IFN response to infection with Mycobacterium tuberculosis requires ESX-1-mediated secretion and contributes to pathogenesis.* J Immunol, 2007. **178**(5): p. 3143-52.

44. Mayer-Barber, K.D., et al., *Host-directed therapy of tuberculosis based on interleukin-1 and type I interferon crosstalk.* Nature, 2014. **511**(7507): p. 99-103.

45. Huet, G., et al., *A lipid profile typifies the Beijing strains of Mycobacterium tuberculosis: identification of a mutation responsible for a modification of the structures of phthiocerol dimycocerosates and phenolic glycolipids.* J Biol Chem, 2009. **284**(40): p. 27101-13.

46. Coscolla, M., *Biological and Epidemiological Consequences of MTBC Diversity.* Adv Exp Med Biol, 2017. **1019**: p. 95-116.

47. Chen, M., et al., *Lipid mediators in innate immunity against tuberculosis: opposing roles of PGE2 and LXA4 in the induction of macrophage death.* J Exp Med, 2008. **205**(12): p. 2791-801.